MISSOURI S&T | CURTIS LAWS WILSON LIBRARY
MISSOURI UNIVERSITY OF SCIENCE AND TECHNOLOGY

Scholars' Mine

Masters Theses | Student Theses and Dissertations

1962

# A model study of the behavior of elastic liners in shallow underground openings

Martin Samuel Oudenhoven

Follow this and additional works at: https://scholarsmine.mst.edu/masters_theses

 Part of the Mining Engineering Commons

Department:

## Recommended Citation

Oudenhoven, Martin Samuel, "A model study of the behavior of elastic liners in shallow underground openings" (1962). *Masters Theses*. 4165.
https://scholarsmine.mst.edu/masters_theses/4165

This thesis is brought to you by Scholars' Mine, a service of the Curtis Laws Wilson Library at Missouri University of Science and Technology. This work is protected by U. S. Copyright Law. Unauthorized use including reproduction for redistribution requires the permission of the copyright holder. For more information, please contact scholarsmine@mst.edu.

www.manaraa.com

T1430

7067

# A MODEL STUDY OF THE BEHAVIOR OF ELASTIC LINERS IN SHALLOW UNDERGROUND OPENINGS

BY

MARTIN S. OUDENHOVEN

---

A

THESIS

submitted to the faculty of the

SCHOOL OF MINES AND METALLURGY OF THE UNIVERSITY OF MISSOURI

in partial fulfillment of the work required for the

Degree of

MASTER OF SCIENCE IN MINING ENGINEERING

Rolla, Missouri

1962

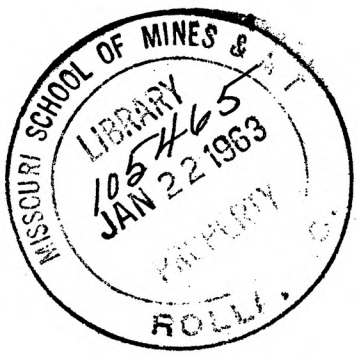


---

Approved by

R. F. Buzenski (advisor) Rodney D. Cudlip

Ray E. Morgan R F Davidson

# ABSTRACT

Models of epoxy resin were used in a stress freezing technique to determine areas of possible failure in lined circular openings. These models were loaded in a centrifuge for a fixed period of time, after which they were analyzed photoelastically. The material characteristic changes, with time, were recorded on graphs and used in the analysis.

Two types of tests were conducted; one, where the lining thickness was changed and, the other, where materials of the liner and plate material were changed.

The resulting analyses furnished proof that the greater the rigidity of the lining, the higher the stress developed in the lining, and also, as the lining thickness increased, holding liner inside diameter constant, the stress decreased in the lining and plate material.

# ACKNOWLEDGEMENTS

The writer is sincerely indebted to Mr. R. F. Bruzewski, Associate Professor of Mining Engineering, University of Missouri, School of Mines and Metallurgy, who offered valuable criticism of this paper, plus advice and assistance in preparing the pictures contained herein.

He also wishes to acknowledge the assistance given him by the members of the mining department. Particular mention is due Mr. R. D. Caudle, Research Instructor, for his aid and advice in adapting the equipment for this investigation.

# TABLE OF CONTENTS

# LIST OF FIGURES

FIGURE NO. PAGE

FIGURE NO. PAGE

# CHAPTER I

## INTRODUCTION

One of the major considerations of an underground opening is its structural stability during the period of its usefulness. In properly supporting such an opening, it is advantageous to eliminate all points of high stress concentrations on its inner surface in order to prevent any minute fracturing which may propagate to total failure. For maximum stability, the shape of the opening must be designed according to the nature of the surrounding stress field and, once determined, it may be preserved by the installation of a concrete lining.

The purpose of this study was to devise an effectual means for comparing and analyzing the resulting stress distributions around openings with and without lining arrangements. This was accomplished by freezing stresses in photoelastic models while under load in a centrifuge. By this means, fixed visual stress patterns were obtained which represented the host rock and lining load conditions for the lining arrangements used. This permitted a leisurely interpretation of the stress patterns and, it is believed, an accurate evaluation of the existing

stress conditions. The final result thus offering, directly and conveniently, information for properly designing similar, circularly shaped concrete liner combinations and, also, for predicting their points of structural failure.

# CHAPTER II

## REVIEW OF THE LITERATURE

A review of the literature on stress analysis of underground openings with concrete linings reveals that the few articles which have been published concern themselves only with mechanical and electrical measurements of deformation.

Early observations and analyses of results from stress fields in lined openings were published in 1949 by Spalding[18]. He discussed the pressure distribution around openings and described specific cases where the lining had failed in shear. Other points presented in his paper dealt with advantages in the elimination of flat surfaces and sharp angles, and the fact that concrete could withstand more compressive stress than tensile and, therefore, the shape should be such that all tensile stresses are minimized.

Four pertinent articles were printed in 1956. Wood[21] introduced the use of Lame's "thick walled cylinder" formula for finding the thickness of a concrete lining by considering the internal radius, admissible stress, and the external pressure,

$$T = R\left(\sqrt{\frac{S}{S-2P}} - 1\right)$$

where: T = Thickness of lining in inches.

R = Internal radius of shaft in inches.

S = Admissible stress in pounds per square inch.

P = External pressure in pounds per square inch.

Gibson[4] gave detailed information on the deformation and strain in two circular Niagara tunnels. Measurement of the stress in the rock before pouring the concrete was accomplished with striding-type deformeters placed at a distance of 25 feet behind the face. Magnetostriction-type stress meters were located at eight equally spaced points around the lining and set three inches in from the inner surface where leads passed to the surface of the ground through old bore holes that were used earlier for conducting raw lining concrete. Results showed that the stress in the lining,after grouting had taken place,was at a maximum seventy days after the initial measurement was made, and dropped to one half that value in an additional seventy days. On the surface of the lining, three points were under tension and none of these exceeded 125 p.s.i. The distribution of the stress was not symmetrical and this was attributed to concrete creep and the decrease in temperature within the tunnel.

A comparison of the methods of analysing stresses in the ground, surrounding underground excavations, was presented by Roux and associates[14]. Advantages and disadvantages of the mathematical and photoelastic methods were discussed. The article states that photoelastic analysis should give solutions for more complex shapes for which mathematical analysis becomes too laborious. This presumeably would include circular openings with linings.

The fourth article, written by Tomkins[19] in 1956, deals with the design of the reinforcement of the concrete lining used in the Cynheidre Mine, England, which was based on Dutch practice. It was pointed out that, at present, the principal difficulty in designing concrete structures at great depths is the lack of reliable information on the magnitude of the ground pressures which may develop. The assumption made was that a destressed area is formed in the shape of an ellipse above an opening. The height of the ellipse was determined by measuring the deflection of the roof before lining. All lined drifts were designed to meet the following conditions:

(a) Full vertical load with no horizontal pressure.

(b) Full horizontal load with no vertical pressure.

(c) Vertical load with horizontal pressure.

(d) Hydrostatic load with 200 feet of water head.

In 1958, Isaacson[9] wrote that, when reinforcing concrete shaft linings, the steel used should run at right angles to the planes of potential shear because, he stated, "The stresses leading to failure will generally be shear stresses".

Research was conducted, in 1959, by Shepherd[16], on the stress in concrete linings with different shaped openings, using vibrating wire strain gauges embedded in concrete tiles. He also examined the junctions of tunnels and shafts because of the concentrations of stresses there.

D. G. Moye[11], in 1959, examined the stress field and other difficulties involved in opening the underground power station in the Snowy Mountains of Australia. Photo-elastic studies were made of the arrangement of multiple openings that were intended to be used. The conclusions that he gave were that these tests plus some drilling for major faulting planes were necessary in the successful location and excavation of a large opening underground.

An article presented by W. T. Moody[10], in 1959, brought a mathematical solution into the problem of stress analysis in rock and concrete linings. The following equation that he put forth was based on Lame's solution for a thick cylinder acted upon by internal hydrostatic pressure:

$$\frac{P_r}{P_c} = \frac{2}{1 + \mu_c + \left(\frac{c}{a}\right)^2 (1 - \mu_c) + \frac{E_c}{E_r}\left(\frac{c^2}{a^2} - 1\right)\left(\frac{b^2 + c^2}{b^2 - c^2} + \mu_r\right)} \qquad (2)$$

where: P = Intensity of radial pressure.

u = Poisson's ratio.

a = Radius to inside of concrete lining.

E = Modulus of elasticity.

b = Effective radius of surrounding rock.

C = Radius to outside of concrete lining.

Subscripts c and r, are used in conjunction with P, u and E, to designate applicability to concrete and rock, respectively. He took into consideration the modulus of elasticity, Poisson's ratio, intensity of radial pressure, and dimensions of various parts of the circular opening and concrete lining as shown in Figure 1. This solution was the first attempt to solve concrete lining problems by considering the various physical properties of the rock and concrete.

Some studies of rock movement in the Niagara Tunnels were presented by Hogg[8] that brought forth the following conclusions which coincided with those of Gibson[4]:

(a) The inward movement in the tunnel was substantial but gave a straight line relationship when plotted on a logarithmic time scale.

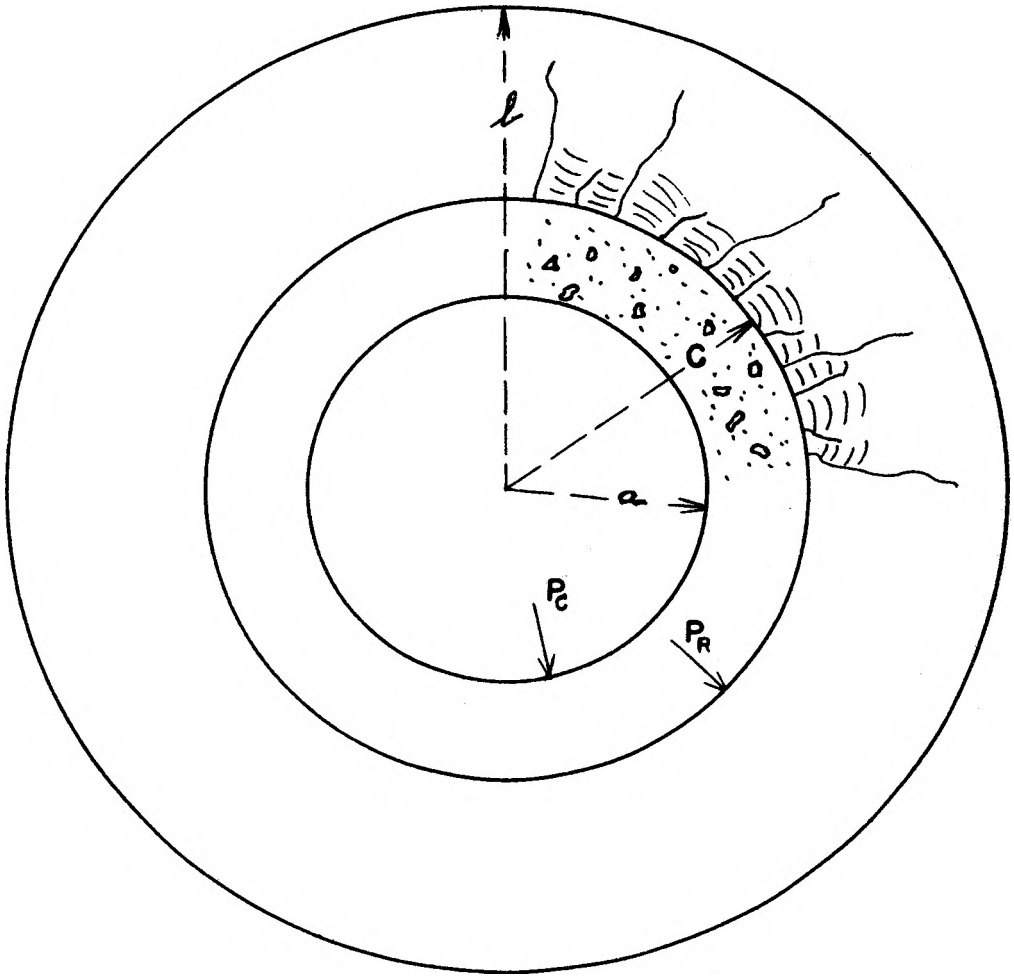


FIG. 1 Circular Opening and
Concrete Lining ( After Moody )

(b) Major inward movement of the wall rock took place in the first few months so that when the concrete was placed, the anticipated movement for the next fifty years was calculated into the useful life.

(c) The project has operated with complete success for about four years and prediction of rock movement for the next fifty years has been made.

In shaft sinking, one of the major problems is the calculation of the required thickness of shaft lining. J. Galanka[3], in 1959, presented an article entitled "Problems of Shaft Sinking in Poland" in which he developed a mathematical formula for calculating the shear stress in a shaft lining. He started with the equation;

$$e = r_w \left( \sqrt{\frac{K}{K - p\sqrt{3}}} - 1 \right) \qquad (3)$$

where, e = Thickness of the lining.

$r_w$ = Internal radius of the shaft.

k = Admissible stress.

p = External pressure.

and developed the following equation for the maximum shear stress:

$$T = \frac{(r + e/2)\, vp}{e - 4\left[\frac{(r + e/2)^3\, p}{Ee^2}\right]} \qquad (4)$$

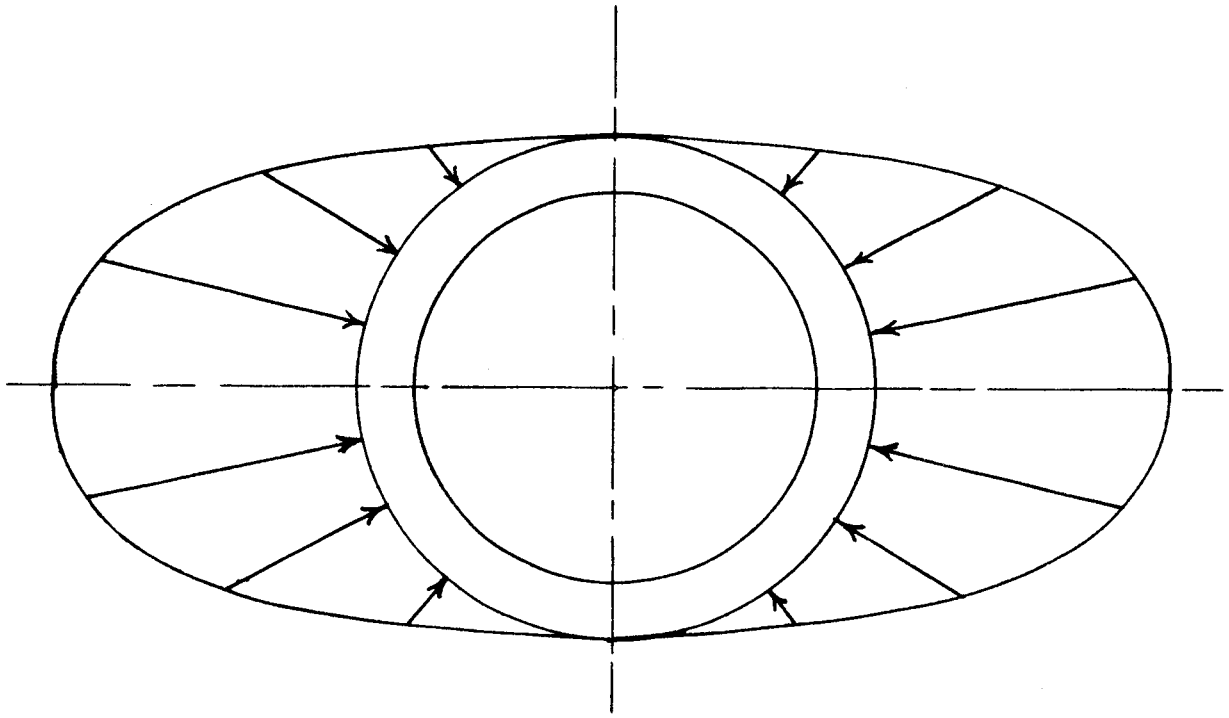

FIG. 2 Earth Pressure $p \cos^2\theta$

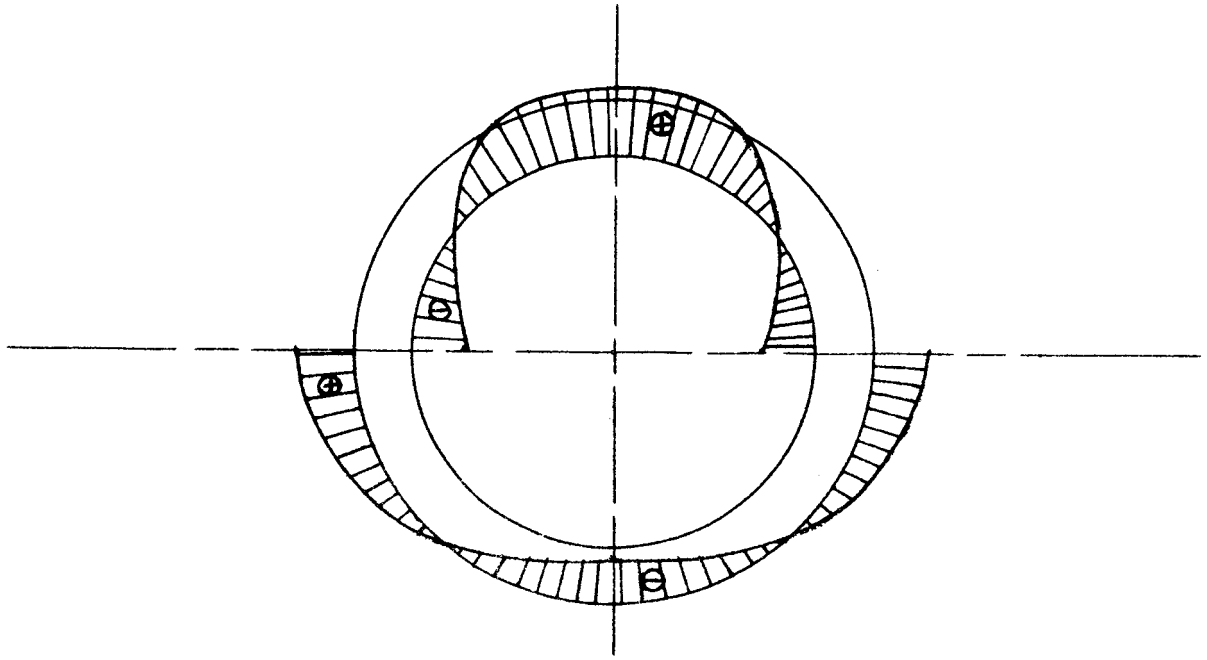


FIG. 3 Results of analysis,
minus signs are tensile stresses

where, T = Maximum shear stress.

p = External pressure.

E = Modulus of elasticity of concrete.

r = Internal radius of the shaft.

e = 5.45 m (for concrete).

m = Maximum eccentricity.

v = The coefficient of variation of the pressure.

A paper entitled "Investigations on the Stress in Circular Shaft Lining" was presented by Y. Hiramatsu and his associates[7] in 1960. They used small photoelastic stress meters of their own design and set these into the concrete, cemented with a hard adhesive. A zero stress field was assumed when the stress meters were installed and the effect of creep, in the concrete, on the stress pattern was not considered but was thought to be small. His conclusions, for the first part of the paper, were that, when lining is used in solid ground, the stress in the lining is almost zero and that most of the stress would come from creep, whereas, in crushed or highly fractured ground, there is frequently high stress. By "highly fractured ground", he presumably means overburden or a large zone of highly fractured rock. The second part of his paper dealt with the theoretical study of the stresses in shaft linings and, by using the theory of elasticity, he derived the following equations for a

horizontal section of a vertical shaft lining subjected to the elliptically distributed pressure, p $\cos^2\theta$ :

$$\sigma_r = \frac{1}{2}\frac{b^2}{b^2-a^2}\left[\left(1-a^2r^{-2}\right)+\frac{1}{(b^2-a^2)}\left\{b^4+b^2a^2+2a^4\right.\right. \tag{5}$$
$$\left.\left.-2a^2\left(2b^4+b^2a^2+a^4\right)r^{-2}+b^2a^4\left(3b^2+a^2\right)r^{-4}\right\}\cos.\,2\theta\right]p$$

$$\sigma_\theta = \frac{1}{2}\frac{b^2}{b^2-a^2}\left[\left(1+a^2r^{-2}\right)+\frac{1}{(b^2-a^2)^2}\left\{2\left(b^2+3a^2\right)r^2\right. \tag{6}$$
$$\left.-\left(b^4+b^2a^2+2a^4\right)-b^2a^4\left(3b^2+a^2\right)r^{-4}\right\}\cos.\,2\theta\right]p$$

$$\tau_{r\theta} = \frac{1}{2}\frac{b^2}{(b^2-a^2)^3}\left\{\left(b^2+3a^2\right)r^2-\left(b^4+b^3a^2+2a^4\right)\right. \tag{7}$$
$$\left.-a^2\left(2b^4+b^2a^2+a^4\right)r^{-2}+b^2a^4\left(3b^2+a^2\right)r^{-4}\right\}(\sin.\,2\theta)p$$

where: b = Outside diameter of the concrete lining.

a = Inside diameter of the concrete lining.

r = Center of the opening to the center of the concrete lining.

p = Earth pressure.

Results of his analysis are shown in Figures 2 and 3. He concluded with the following four points:

(a) When point loads act on a lining, the original stress may increase 15 to 60 times.

(b) Using an elliptical opening, the maximum compressive and tensile stresses are about 1/2.5 to 1/3 times those resulting from diametrically opposite point loads.

(c) As the thickness of the lining increases, the maximum compressive and tensile stresses decrease.

(d) As the number of maximum stress points increase, the maximum stress per point decreases.

Investigations were conducted into the problem of stress distribution in and around lined vertical mine shafts by G. N. Savin[15], in 1961. The significant difference between his work and that of the investigators discussed previously was that hydrostatic free-field stresses were used in the analysis rather than assumed pressure distributions on the exterior of the linings. Four specific examples of rock and concrete liner combinations were developed. He also made a mathematical analysis of the stresses in a plate, in tension, containing a circular hole into which an elastic ring was inserted. The equations given separately for the stresses in the ring and in the plate are shown in Figure 4. The applicability of these equations to the problem of a lined tunnel in a uniaxial stress condition will be investigated in Chapter III.

$$\sigma_r = \frac{\rho}{2}\left[\left(a_1 - \frac{b_{-1}}{2}\cdot\frac{R^2}{r^2}\right) + \left(\frac{b_1}{2} - 2a_{-1}\frac{R^2}{r^2} - \frac{3}{2}b_{-3}\frac{R^4}{r^4}\right)\cos 2\theta\right]$$

$$\sigma_\theta = \frac{\rho}{2}\left[\left(a_1 + \frac{b_{-1}}{2}\cdot\frac{R^2}{r^2}\right) - \left(\frac{b_1}{2} - 6a_3\frac{r^2}{R^2} - \frac{3}{2}b_{-3}\cdot\frac{R^4}{r^4}\right)\cos 2\theta\right]$$

$$\tau_{r\theta} = \frac{\rho}{2}\left[3a_3\cdot\frac{r^2}{R^2} - \frac{b_1}{2} - a_{-1}\cdot\frac{R^2}{r^2} - \frac{3}{2}b_{-3}\frac{R^4}{r^4}\right]\sin 2\theta$$

Stresses in the elastic ring

$$\sigma_r = \frac{\rho}{2}\left[\left(1 - \frac{1}{2}\beta_{-1}\cdot\frac{R^2}{r^2}\right) + \left(1 - 2\alpha_{-1}\cdot\frac{R^2}{r^2} - \frac{3}{2}\beta_{-3}\cdot\frac{R^4}{r^4}\right)\cos 2\theta\right]$$

$$\sigma_\theta = \frac{\rho}{2}\left[\left(1 + \frac{1}{2}\beta_{-1}\frac{R^2}{r^2}\right) - \left(1 - \frac{3}{2}\beta_{-3}\frac{R^4}{r^4}\right)\cos 2\theta\right.$$

$$\tau_{r\theta} = -\frac{\rho}{2}\left(1 + \alpha_{-1}\cdot\frac{R^2}{r^2} + \frac{3}{2}\beta_{-3}\cdot\frac{R^4}{r^4}\right)\sin 2\theta$$

Stresses in the plate

$$a_{-1} = \frac{2(1+\chi)}{D_1}\left[\left(\frac{\mu}{\mu_1} - 1\right) + m^6\left(1 + \chi_1\frac{\mu}{\mu_1}\right)\right]$$

$$a_1 = \frac{m^2(1+\chi)}{2\left(\frac{\mu}{\mu_1} - 1\right) - m^2\left[\left(\frac{\mu}{\mu_1} - 1\right) - \left(1 + \chi_1\frac{\mu}{\mu_1}\right)\right]}$$

$$a_3 = -\frac{2(1+\chi)}{D_1}m^4(m^2-1)\left(\frac{\mu}{\mu_1} - 1\right)$$

$$b_{-3} = -\frac{2(1+\chi)}{D_1}\left[\left(\frac{\mu}{\mu_1} - 1\right) + m^4\left(1 + \chi_1\frac{\mu}{\mu_1}\right)\right]$$

$$b_{-1} = \frac{2(1+\chi)}{2\left(\frac{\mu}{\mu_1} - 1\right) - m^2\left[\left(\frac{\mu}{\mu_1} - 1\right) - \left(1 + \chi_1\frac{\mu}{\mu_1}\right)\right]}$$

$$\beta_{-1} = 2 - \frac{2(m^2-1)(1+\chi)}{2\left(\frac{\mu}{\mu_1} - 1\right) - m^2\left[\left(\frac{\mu}{\mu_1} - 1\right) - \left(1 + \chi_1\frac{\mu}{\mu_1}\right)\right]}$$

FIG. 4

$$b_1 = \frac{2(1+\chi)}{D_1}\left[\left(\frac{\mu}{\mu_1}-1\right)(4-3m^2)+m^6\left(1+\chi_1\frac{\mu}{\mu_1}\right)\right]m^2$$

$$\alpha_{-1} = 2-\frac{2(1+\chi)}{D_1}\left[\left(\frac{\mu}{\mu_1}-1\right)(3m^6-6m^4+4m^2-1)+m^6(m^2-1)\left(1+\chi_1\frac{\mu}{\mu_1}\right)\right]$$

$$\beta_{-3} = -2+\frac{2(1+\chi)}{D_1}\left[\left(\frac{\mu}{\mu_1}-1\right)(4m^6-7m^4+4m^2-1)+m^4(m^4-1)\left(1+\chi_1\frac{\mu}{\mu_1}\right)\right]$$

$$D_1 = \left(\chi+\frac{\mu}{\mu_1}\right)m^2\left[\left(\frac{\mu}{\mu_1}-1\right)(3m^4-6m^2+4)+m^6\left(1+\chi_1\frac{\mu}{\mu_1}\right)\right]$$
$$+\left(\chi_1\frac{\mu}{\mu_1}-\chi\right)\left[\left(\frac{\mu}{\mu_1}-1\right)+m^6\left(1+\chi_1\frac{\mu}{\mu_1}\right)\right]$$

$$m = \frac{R}{r}$$

$$\mu_1 = \frac{E}{2(1+\nu_1)}$$

$$\mu = \frac{E}{2(1+\nu)}$$

$$\chi_1 = \frac{3-\nu_1}{1+\nu_1}$$

$$\chi = \frac{3-\nu}{1+\nu}$$

WHERE,

r = Radius, inside of the opening
R = Radius to the outside of the lining
$\nu$ = Poisson's ratio, plate material
$\nu_1$ = Poisson's ratio, lining material
$\mu$ = Modulus of Rigidity, plate material
$\mu_1$ = Modulus of Rigidity, lining material

Constants

FIG. 4 Equations for the stresses in the vicinity of a hole in a plate reinforced by an elastic ring, subjected to a uniaxial stress, P.

H. Shimada[17] investigated photoelastically the stress distribution in epoxy resin bars, containing circular openings reinforced by aluminum rings, under uniaxial tension. The relevance of his results to the present study will also be shown in Chapter III.

A non-dimensional equation for the stresses in a gravitating elastic body subjected to external forces was used by Panek[13] in which;

$$\frac{\sigma}{WL} = f\left[\frac{WL}{E}, \frac{\rho}{EL^2}, \frac{t}{L}, \frac{b}{L_1}, \ldots, \frac{x}{L}, \frac{y}{L}, \frac{z}{L}, \frac{E'}{E}, \frac{E''}{E}, \ldots \mu, \mu'\right] \quad (14)$$

In the case of composite model tests in the centrifuge, where no independent external forces are applied, and where the dimensional proportions of the prototype are maintained, this equation can be simplified, giving;

$$\frac{\sigma}{WL} = f_2\left[\frac{WL}{E}, \frac{E'}{E}, \mu, \mu'\right] \quad (15)$$

where: $\sigma$ = The stress at any point

w = The unit weight

L = Some pertinent dimension

E = Modulus of Elasticity

E' = Modulus of a second material

$\mu$ = Poisson's ratio

$\mu'$ = Poisson's ratio of a second material

Panek shows that if the following relationships are satisfied:

$$\frac{w_{m_{eff}} L_m}{E_m} = \frac{w_p L_p}{E_p} \tag{16}$$

$$\frac{E'_m}{E_m} = \frac{E'_p}{E_p} \tag{17}$$

$$\mu_m = \mu_p \tag{18}$$

$$\mu'_m = \mu'_p \tag{19}$$

where subscripts m and p are used to designate model and prototype, respectively,

the stresses developed in the model must bear the following relationship to those in the prototype:

$$\frac{\sigma_m}{E_m} = \frac{\sigma_p}{E_p} \tag{20}$$

Equation (16) cannot normally be satisfied by a model in a gravitational field, where $w_m = w_{m_{eff}}$. Therefore, the use of centrifugal forces to simulate the gravitational loading of the prototype was suggested by

Panek[13], and thus equation (16) becomes;

$$\frac{Kw_m L_m}{E_m} = \frac{w_p L_p}{E_p} \text{ , where } K = \frac{4\pi r N^2}{g} \qquad (21)$$

$$\text{or, } Kw_m = n \frac{E_m}{E_p} W_p \text{ , where the scale factor, } n = \frac{L_p}{L_m} \qquad (22)$$

$$\text{thus, } n = \frac{Kw_m E_p}{w_p E_m} \qquad (23)$$

where, r = Radius of circle.

N = Number of revolutions per second.

g = Acceleration due to gravity.

In considering the dependence of stress distribution on elastic constants, M. Clutterbuck[1], in 1957, quoted Muskhelishvili, "The same stress functions (and therefore the same stresses) will give the solution for the distribution of stress for bodies of different materials with different values of Poisson's ratio if, and only if, the resultant vectors of the external forces applied to each boundary of the body separately are zero, then, and only then, the state of stress does not depend on the elastic constants". He further stated that for a given geometrical shape loaded in a given manner, the stress in a model of a single given material divided by some relevant nominal stress is a non-dimensional quantity (stress concentration factor). Since this quantity involves the elastic con-

stants, it must involve them in a non-dimensional manner, implying that the stress concentration factors are a function of Poisson's ratio only. He found in an experimental investigation of a loaded hole in an infinite plate that a change in stress concentration factor due to a change in the value of Poisson's ratio was of an order not greater than that of the errors of observation, that is, about 7%.

All references which follow in this chapter are concerned with the explanation and interpretation of the methods used in this study.

In the analysis of stresses around underground openings without linings, Obert[12] presents graphs, Figure 5, that indicate where and how great the stress change is around a circular opening with a unidirectional stress field. The fringe patterns, from a photoelastic analysis and which represent lines of maximum shear, can be compared with theoretical curves of stress distribution such as those of Obert to substantiate data obtained from model studies of simple, circular underground openings.

Walker[20], in a detailed paper, gives the parameters which, when varied, affect the modulus of elasticity of concrete. An estimate of the average modulus of elasticity that concrete may have when these parameters are varied is given in a group of charts. An average

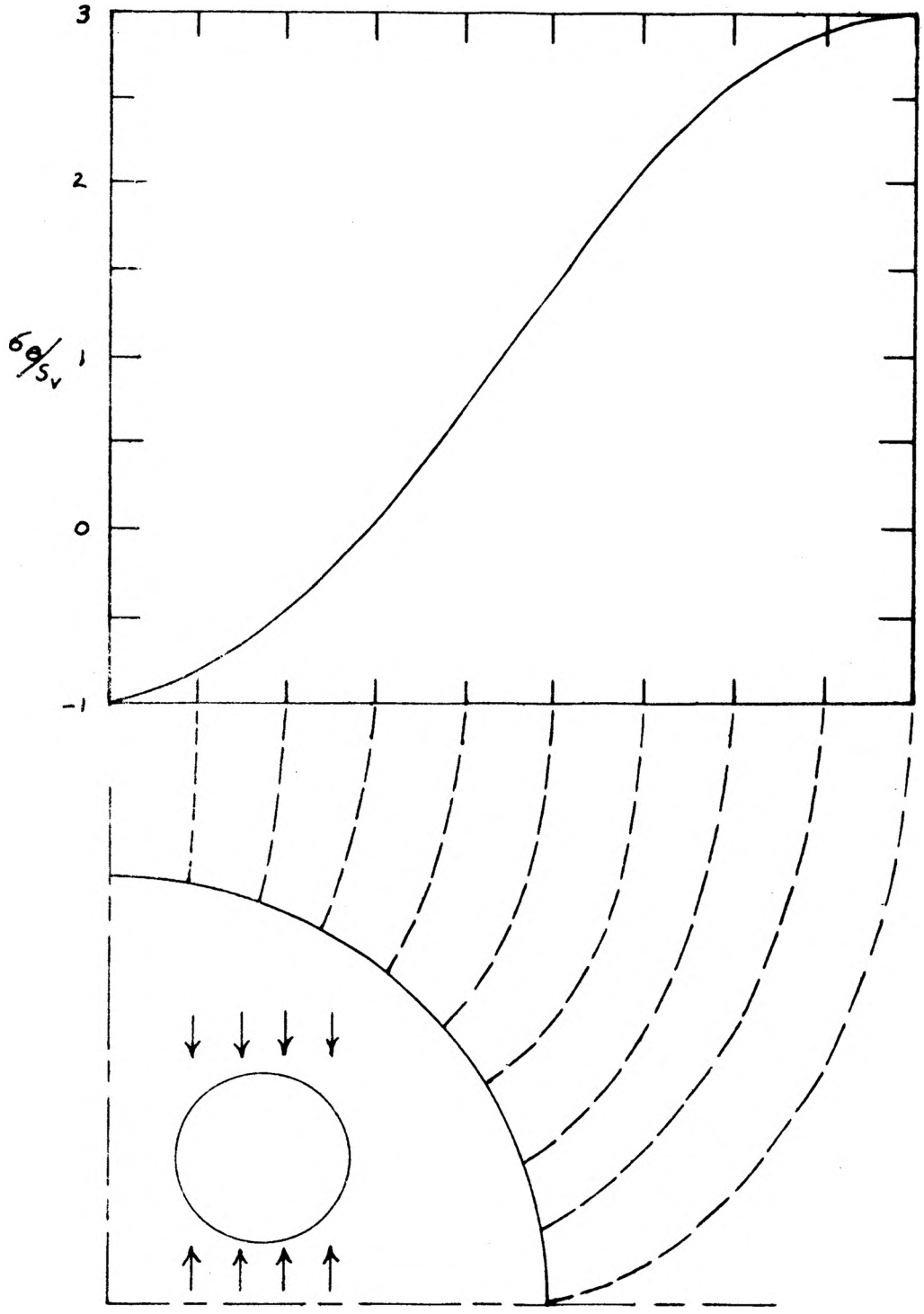


FIG. 5 Unidirectional Stress Field

modulus for concrete, taken from this article and compared to an average modulus for the rock described by Isaacson, is the basis for the ratio used in this study.

When a reduced-scale model is used to study an actual structure, it is necessary that the model be designed so that full-scale behavior of the prototype may be deduced from the observations of the behavior of the model. To accomplish this, the dimensions of the model and characteristics of the material must bear certain relations to the dimensions and material of the prototype.

It is often desirable to use a material which has a lower modulus of elasticity than the material of the prototype so that the forces which are applied to distort the model may be small. The selection of the scale of a model depends upon the properties of the material and the size and type of equipment used. As the scale of the model is reduced, it becomes more difficult to maintain exact geometric similarity.

In analyzing models photoelastically, different methods are given by Hetenyi[6] for determining the stress optic constant and the modulus of elasticity of the material used. This is taken up in detail, along with other related points, later in the chapter on experimental procedure.

The method of "locking-in" stresses in photoelastic materials is described in an article by Dally[2]. He used a modified epoxy resin, molded in aluminum and cured for 12 to 16 hours in a water bath at 70 degrees Fahrenheit. The models were loaded in a 10 foot diameter centrifuge and rotated at 300 R.P.M. for three hours. A grid, molded into the model, was used to determine the stress distribution. It was found that creep took place after unloading the model but, at the end of the curing period, an equilibrium point is reached and the remaining distortions are locked in. His conclusion was that this method seemed well suited for application to the solution of gravitational problems.

D. Haber[5], in 1962, worked with the same epoxy resin that Dally used. In his Master of Science thesis, he describes the results of his studies of the stress distribution around circular openings when using multi-layered photoelastic material. Many of Haber's techniques of casting and preparing the resin were found useful in this work, even though the stress freezing technique was not used in his investigation because the chemical, cyclo-hexanol, when used as a thinner or plasticiser, created tension cracks in the resin after 24 hours.

# CHAPTER III

## EXPERIMENTAL PROCEDURE

An experimental procedure was developed for the fabrication of photoelastic models consisting of thin epoxy resin plates containing single circular holes with epoxy liners. The elastic properties of liners and plates and liner thicknesses were varied to determine the effect of these parameters upon the stress distribution in the models when loaded by centrifugal forces.

The study was facilitated by using a suitable photoelastic model material, an appropriate model holder and loading device, and the necessary instrumentation for analyzing results.

### Model Material

In selecting a suitable elastic material for a model, certain principles, established by the theory of elasticity, were used as a guide. First, the material had to be perfectly elastic; second, strains developed had to be small; and, third, the material had to be isotropic and homogeneous.

A model of an epoxy resin would meet all of these requirements if all of its components were of one material. However, in this study, two materials with differing characteristics were used and, therefore, only the individual components of the model were homogeneous and isotropic.

The photoelastic material used for the models was a clear organic, epoxy resin, commercially called Araldite 502. It is a liquid at normal temperatures which, upon mixing with a plasticiser (dibutyl phthalate) and a hardner (HN-951), solidifies into a soft plastic within 12 to 20 hours. An exothermic reaction takes place during curing and, therefore, when using large concentrated quantities (i.e., plate thicknesses of more than ½ inch), care must be taken to provide adequate methods of cooling.

The major chemical reaction takes place within the first hour or so after adding the hardener and continues, in the mixture used by Dally, at a decreasing rate for approximately 20 hours. The time of hardening varies inversely as the amount of hardener used. However, in using higher ratios of hardener to resin, such as 2 to 9, residual stresses appear in the model as the hardening time is shortened. All modified epoxy resins used in this study could be machined, after curing for 11 hours, without leaving traces of residual stresses. The material characteristics of the resins changed continually during the

a. Prepared Mold
b. Prepared Resin and Poured
c. Resin Curing
d. Machined Lining and Placed in Mold
e. Prepared Second Resin
f. Curing Time for the Second Resin
g. Prepared and Weighed Model and Model Holder
h. Evacuated Tank
i. Started Centrifuge and held at a Constant Speed
j. Took out Model

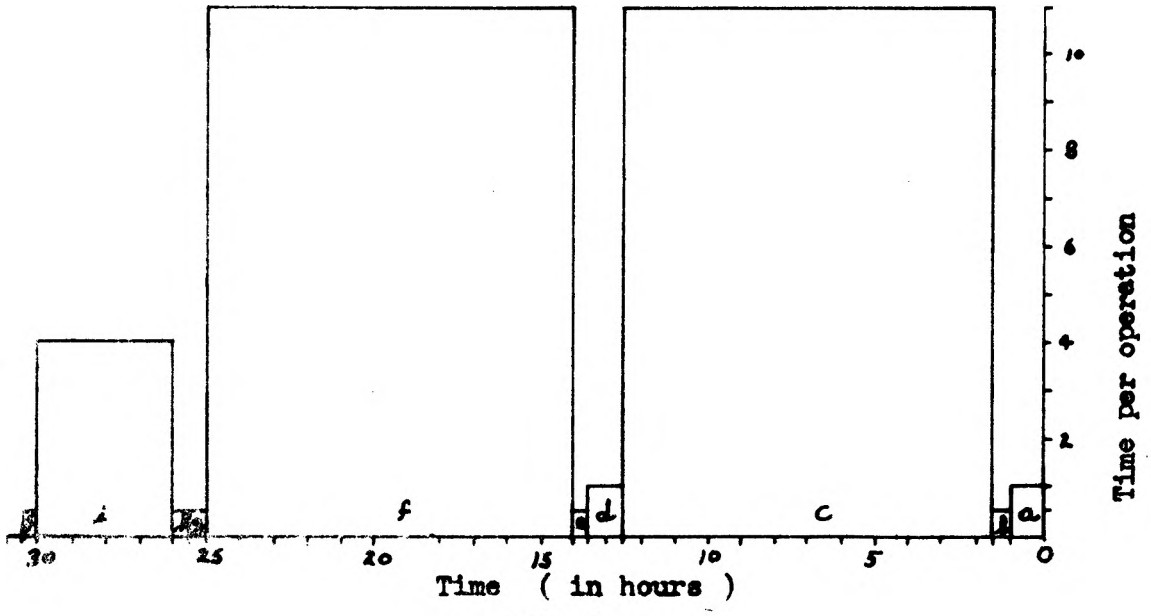


FIG. 6

Time Distribution Chart

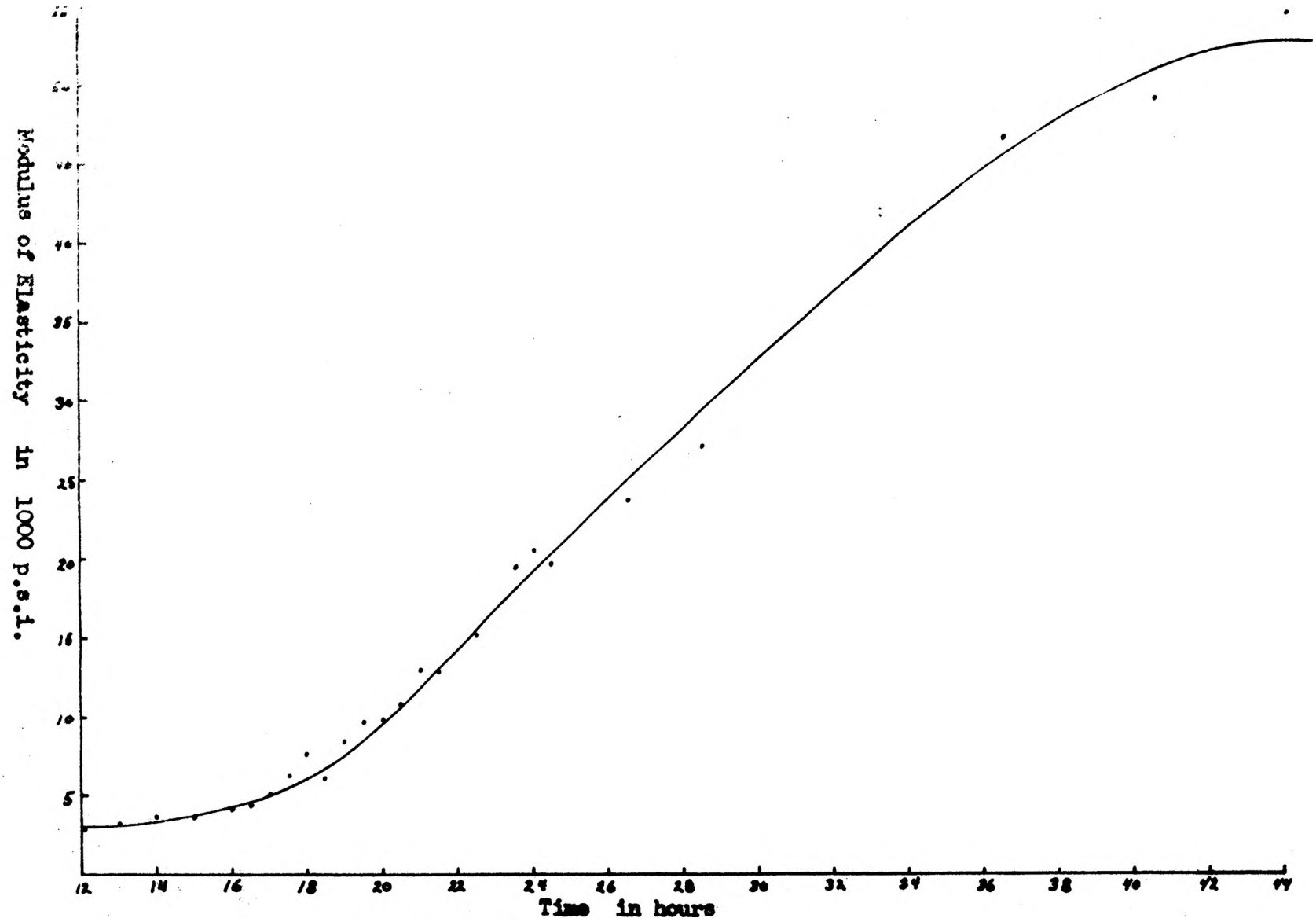


FIG. 7 Modulus of Elasticity vs. Time, Resin 72/20/8, Controlled

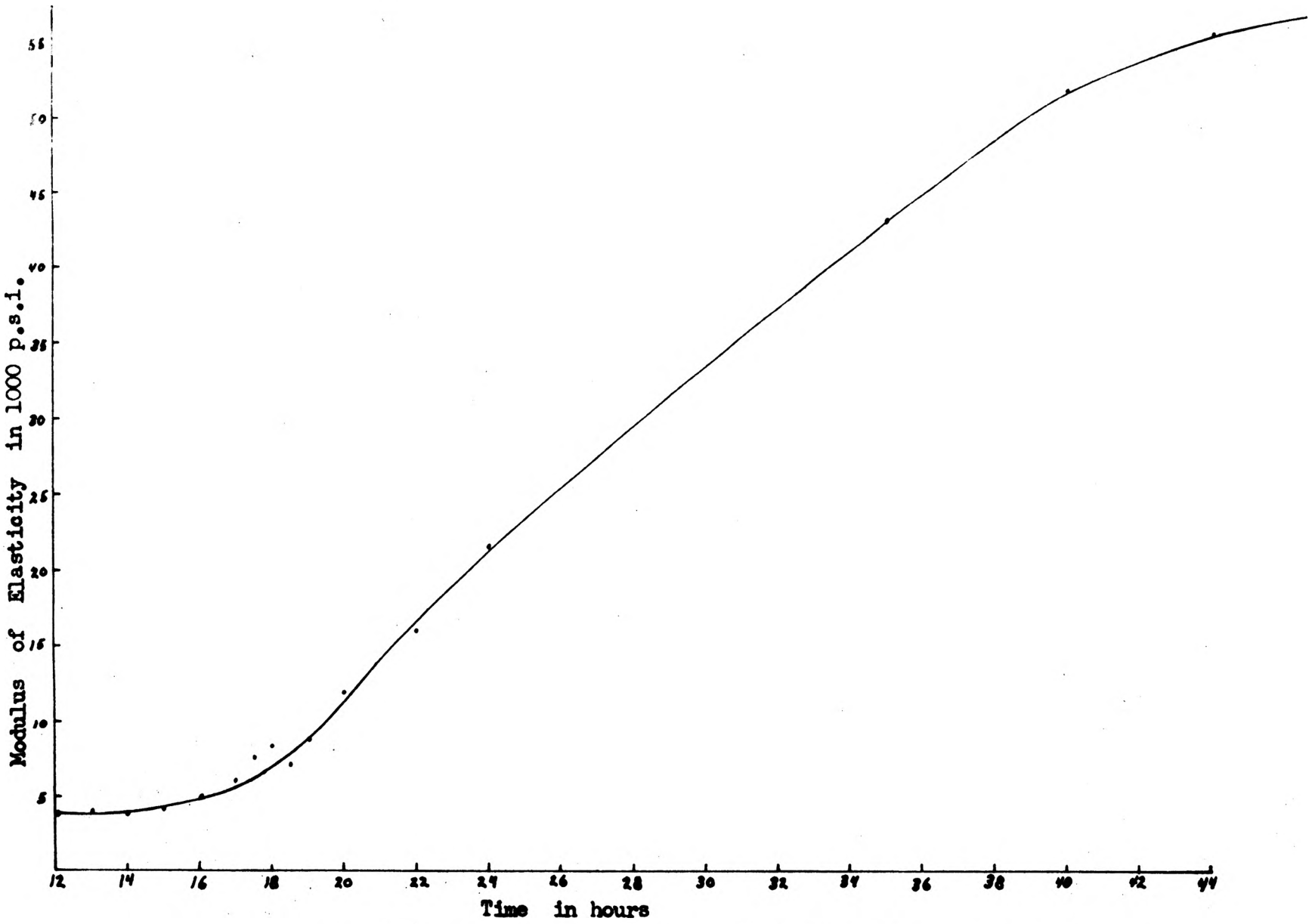


FIG. 8 Modulus of Elasticity vs. Time, Resin 72/20/8, Uncontrolled

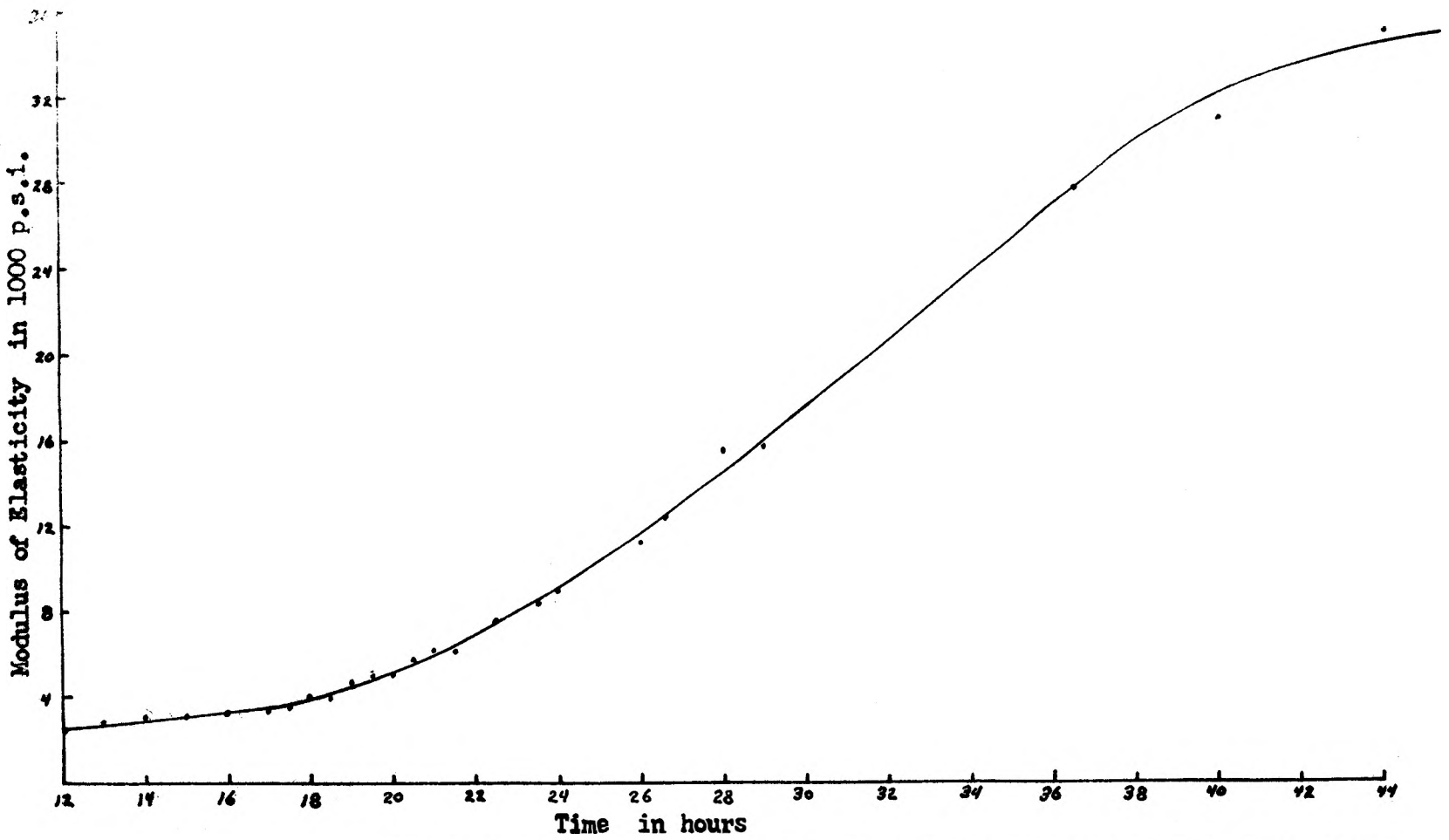


FIG. 9 Modulus of Elasticity vs. Time, Resin 72.4/ 20.1/ 7.5, Controlled

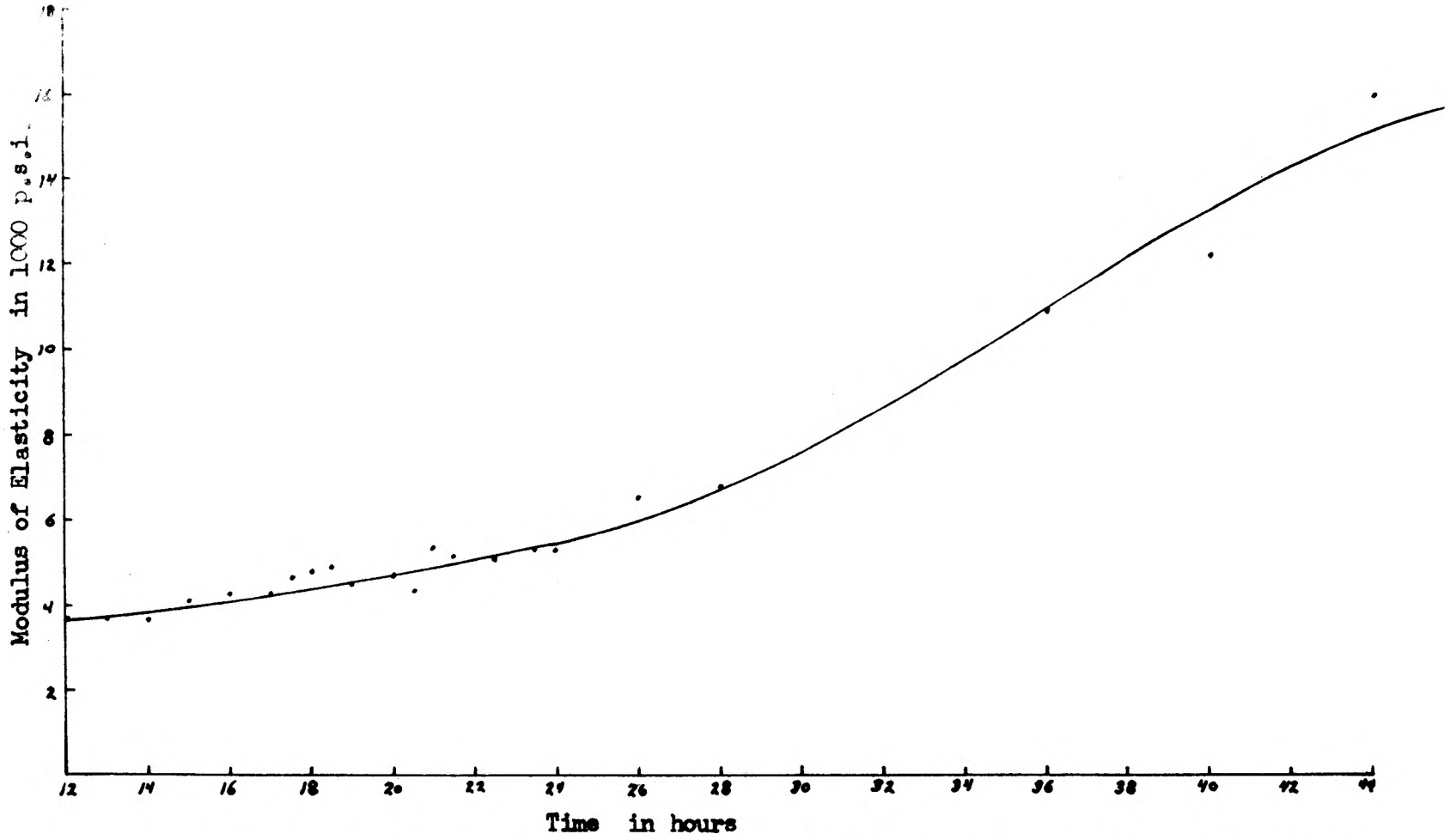


FIG. 10 Modulus of Elasticity vs. Time, Resin 72.7/20.2/7.1, Controlled

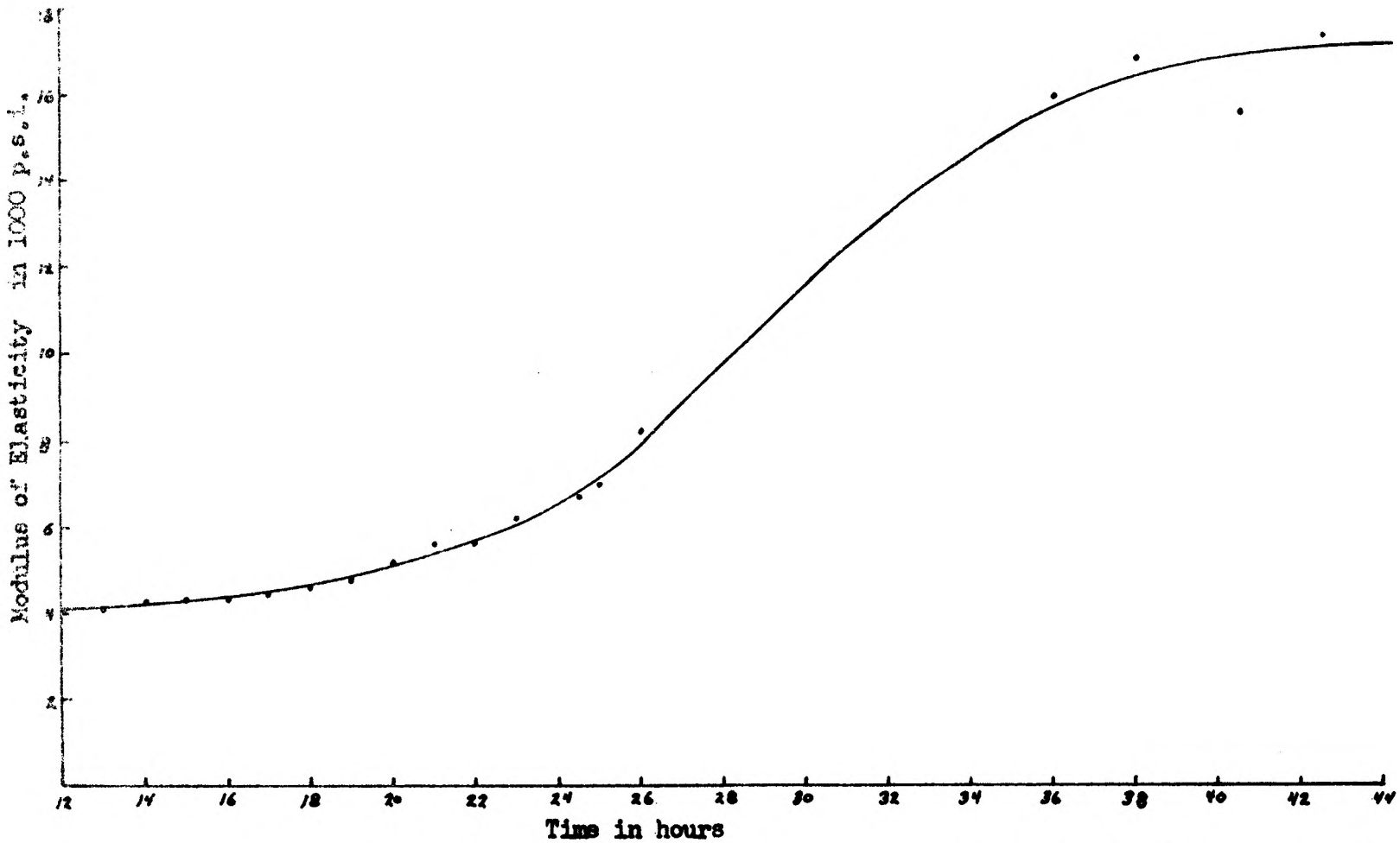


FIG. 11 Modulus of Elasticity vs. Time, Resin 72.7/20.2/7.1, Uncontrolled

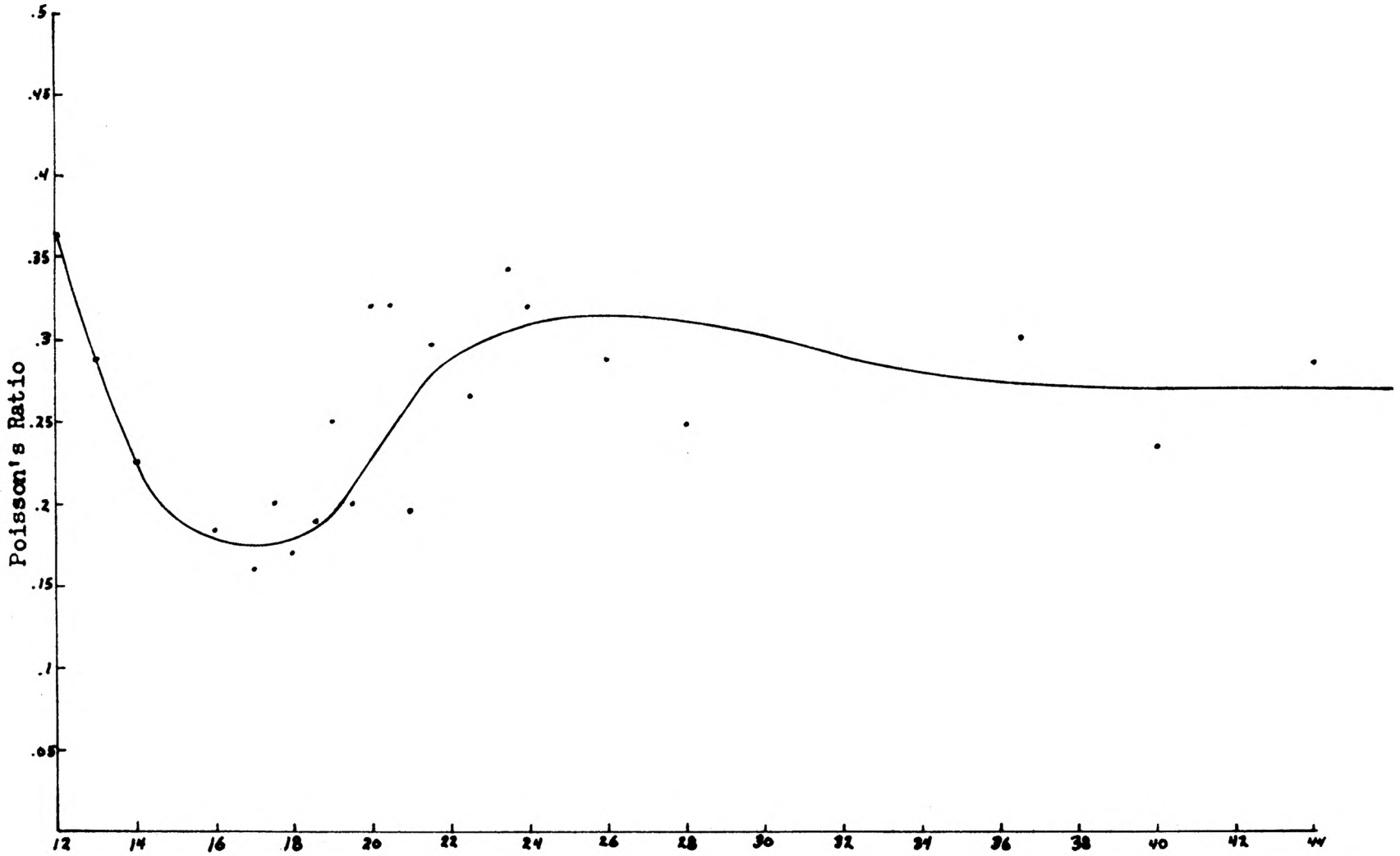


FIG. 12 Poisson's Ratio vs. Time, Resin 72.4/20.1/7.5, Controlled

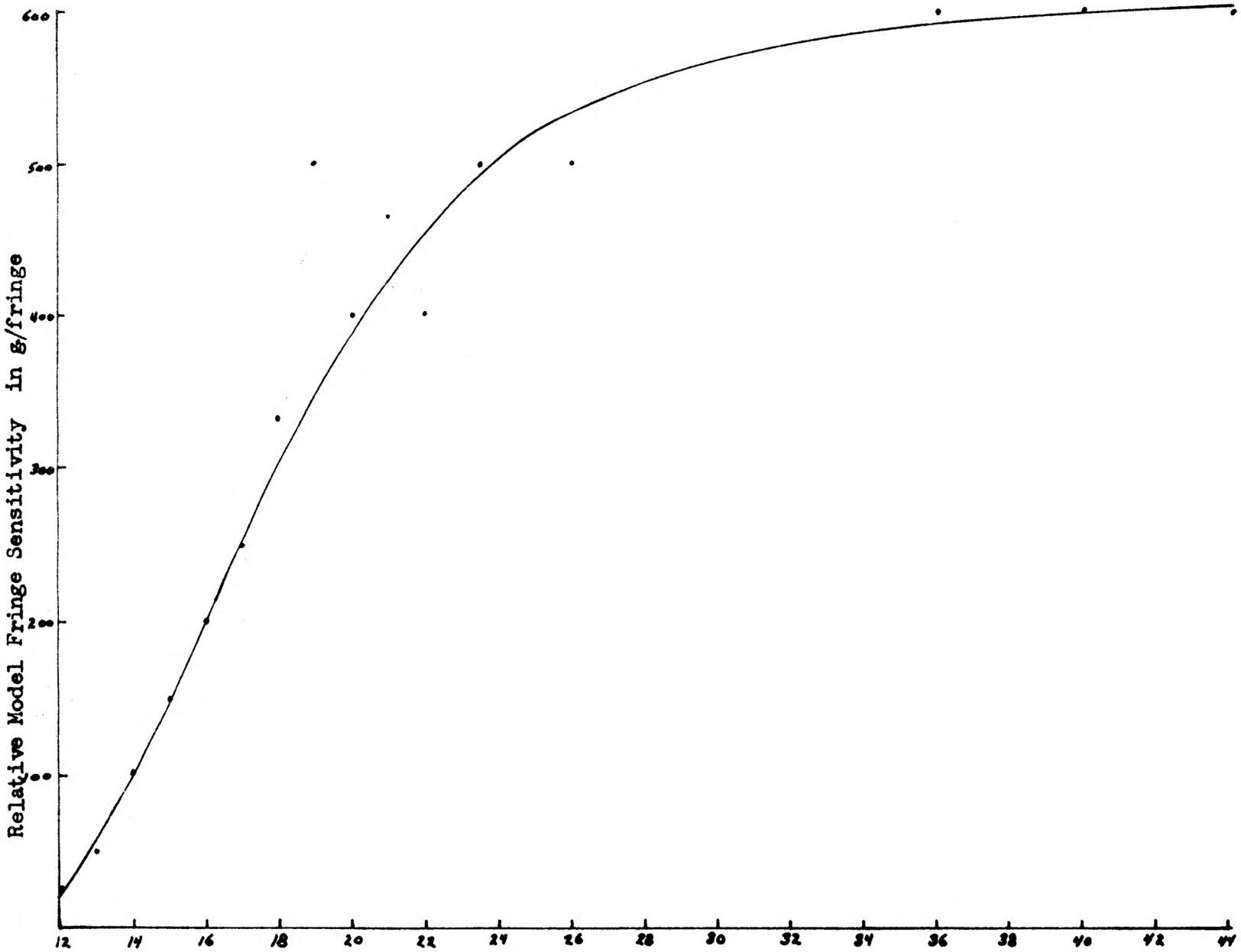


FIG. 13 Relative Fringe Sensitivity vs. Time, Resin 72/20/8, Controlled

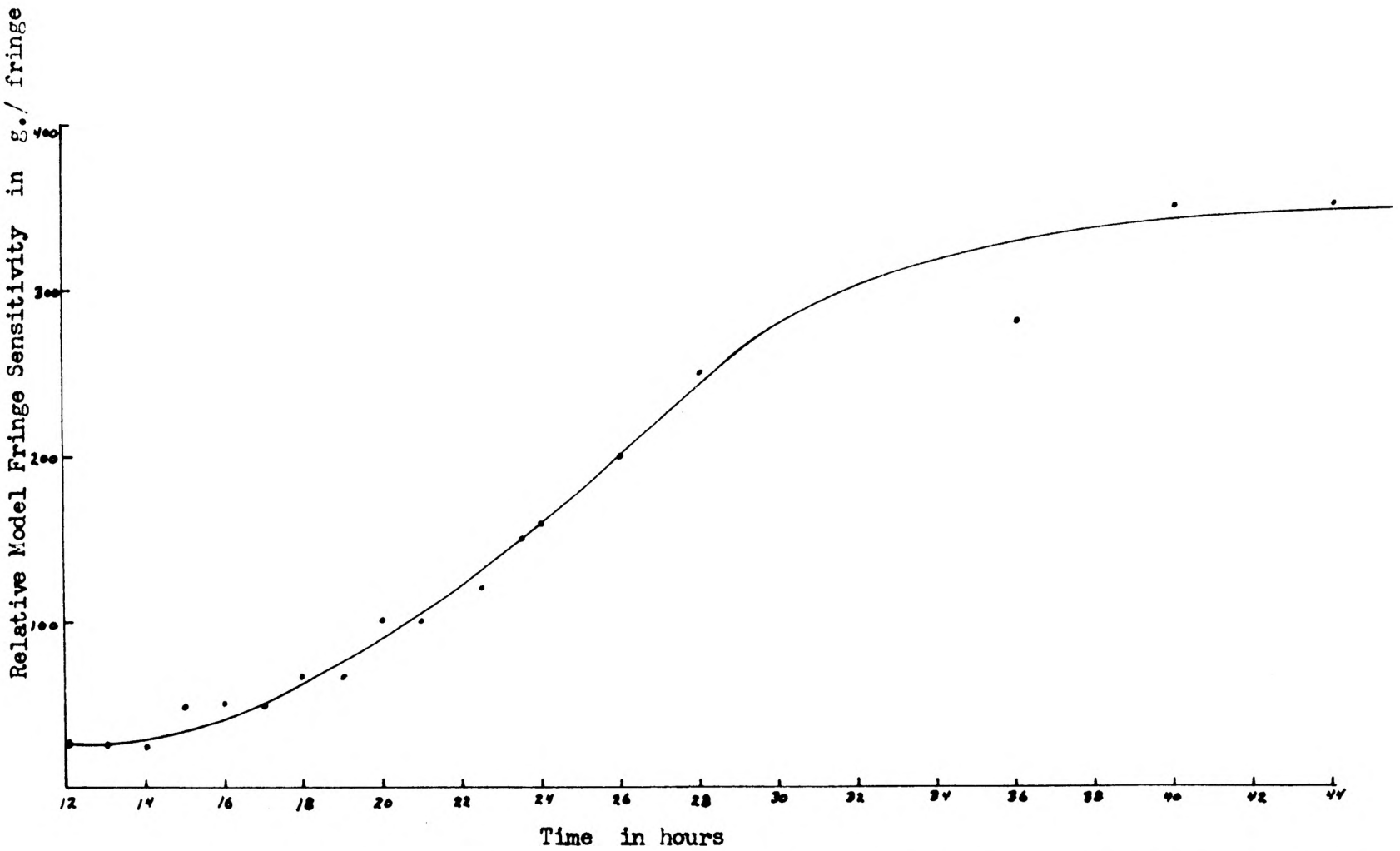


FIG. 14 Relative Fringe Sensitivity vs. Time, Resin 72.7/20.2/7.1, Controlled

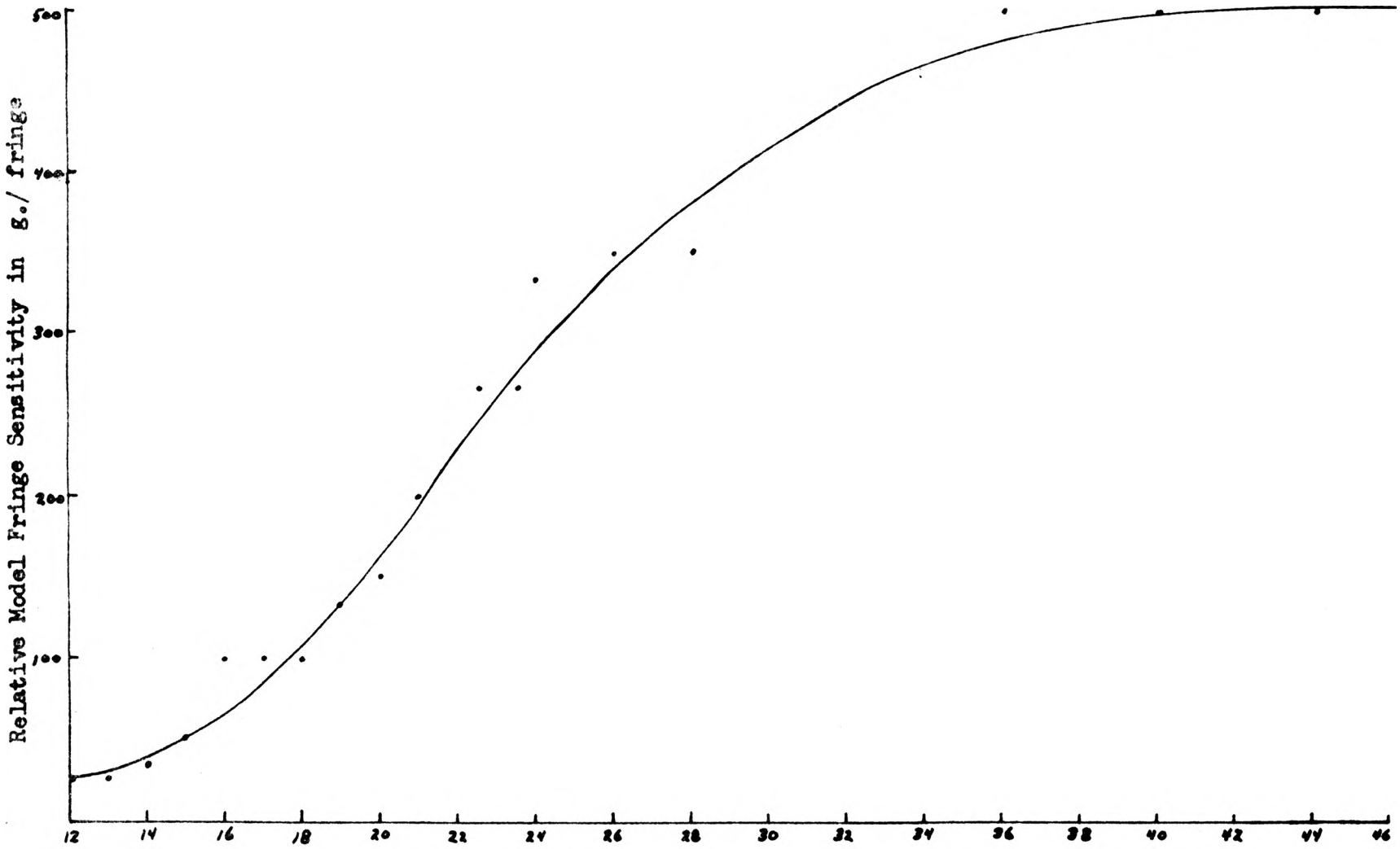


FIG. 15 Relative Fringe Sensitivity vs. Time, Resin 72.4/20.1/7.5, Controlled

| Test No. | Fig. No. | Material | | Model Dimensions (in.) | | | Curing Time (at loading) | | Modulus of Elasticity (+2hr.) | | (in.) Lining Thickness |
|---|---|---|---|---|---|---|---|---|---|---|---|
| | | Plate | Lining | Width | Thickness | Height | Plate (hr) | Lining (hr) | Plate (in p.s.i.) | Lining (p.s.i.) | |
| 1 | | A | —— | 8.875 | 0.5 | 8.0 | 14.25 | ------- | 4,450. | ——— | 0.0 |
| 2 | 28-A | A | —— | | | | 12.75 | ------- | 3,750. | ——— | 0.0 |
| 3 | 29-A | C | A | | | | 12.5 | 25.5 | 3,850. | 27,250. | 0.226 |
| 4 | 30-A | A | A | | | | 12.25 | 26.25 | 3,550. | 29,000. | 0.226 |
| 5 | 31-A | A | B | | | | 13.0 | 30.0 | 3,800. | 20,500. | 0.226 |
| 6 | 32-A | A | C | | | | 12.75 | 26.25 | 3,750. | 6,850. | 0.226 |
| 7 | 33-A | A | B | | | 8.226 | 12.35 | 26.35 | 3,590. | 15,100. | 0.452 |
| 8 | 34-A | A | B | | | 8.452 | 12.55 | 24.55 | 3,630. | 12,300. | 0.678 |
| 9 | 35-A | A | B | | | 8.678 | 12.15 | 24.15 | 3,530. | 11,850. | 0.904 |

where, A = 72%, 20%, 8%
B = 72.4%, 20.1%, 7.5%
C = 72.7%, 20.2%, 7.1%

FIG. 16 Model Property Chart

hardening period.

The procedure of molding and stressing the two different epoxy resins, which were used in each composite model tested, required a total time of at least 30 hours. Figure 6 shows how this time was utilized and, also, it illustrates the importance of uninterrupted scheduling of events. Any delay in the normal procedure would cause an increase in the curing time of the resins and thus, in turn, alter their moduli of elasticity, Poisson's ratio and fringe values from those of a normal test. This would pose difficulties in comparing results of the various tests undertaken. For this reason, a series of hourly determinations were made, of the material characteristics of each model composition, during a complete 44-hour curing period. These data were then plotted graphically (Figures 7 through 15) and utilized in ascertaining model characteristics, at any stage of curing, for making "corrected" comparisons of test data. A record of pre-test curing times and model compositions and dimensions were tabulated in Figure 16 to facilitate using the graphs.

The modulus of elasticity and Poisson's ratio of each composition were determined from SR-4 electric strain gages embedded in cylindrical specimens of the plastic (Figure 18). Strain was measured on a Hathaway Strain Indicator in micro-inches per inch.

In calculating the modulus of elasticity, the following equations were used:

$$E = \frac{s}{e} \quad , \quad s = \frac{P}{a}$$

where, s = stress

P = load

a = area

e = strain

E = modulus of elasticity

Figure 17 summarizes the results of ten tests of stress vs. strain for one epoxy resin mixture at 12 hours curing time. The modulus of elasticity was determined from the straight line fitted to these plotted data and appears quite consistent. Other values of Young's modulus for the plastics used in these experiments ranged from 3000 to 40,000 psi.

An accurate determination of Poisson's ratio proved to be difficult. It appeared that the embedded strain gages used in measuring deformations were slightly warmed by the electrical current passing through them, resulting in a change in their resistance, and they also warmed the surrounding specimen material causing a change in its elastic properties. Furthermore, the exothermic chemical reaction of the specimen material further warmed the strain gages. This combination of circumstances undoubtedly injected an indeterminate error. On the other hand, Poisson's ratio,

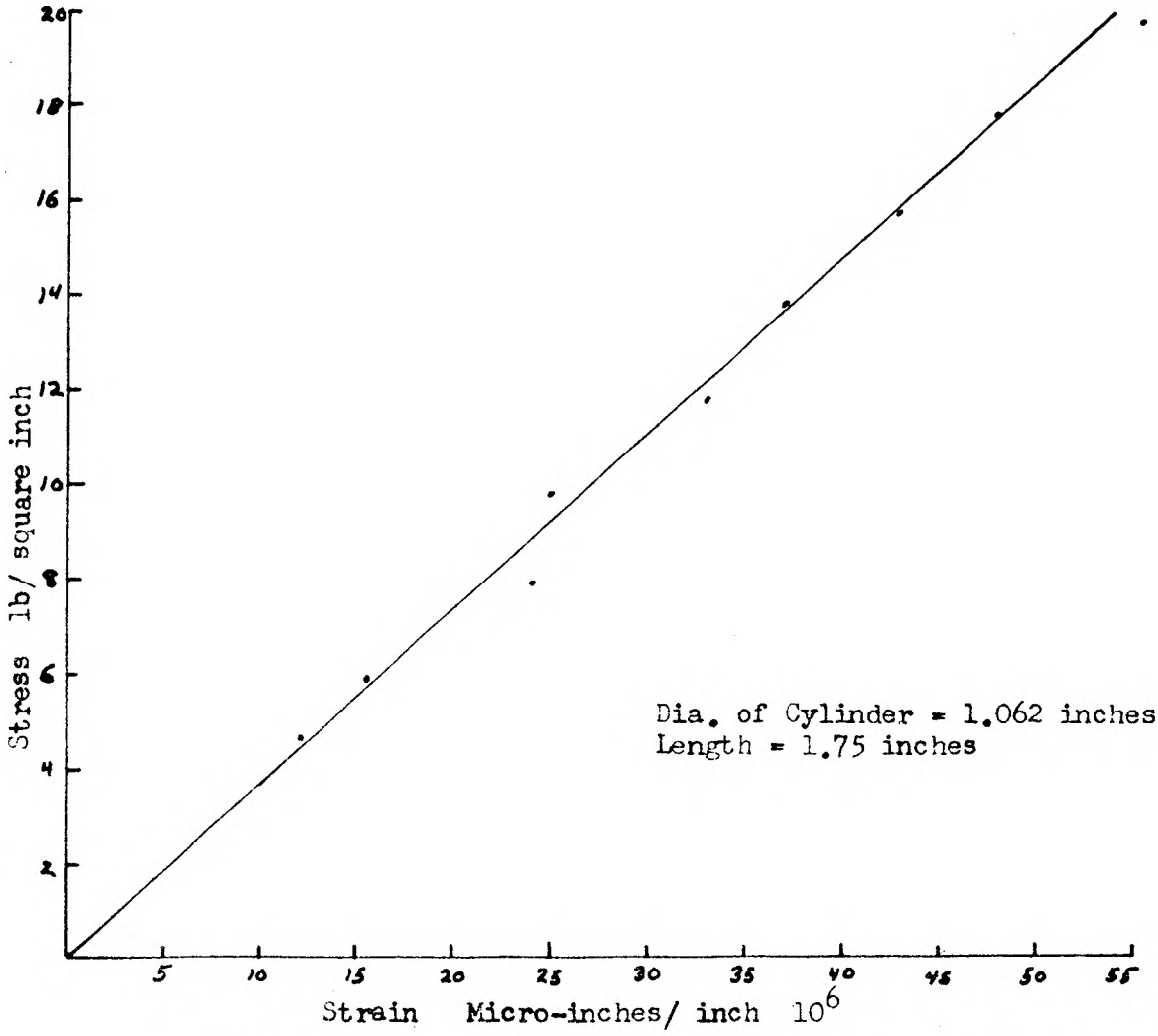


FIG. 17 Stress vs. Strain, Resin 72.7/20.2/7.1, at 12 hours

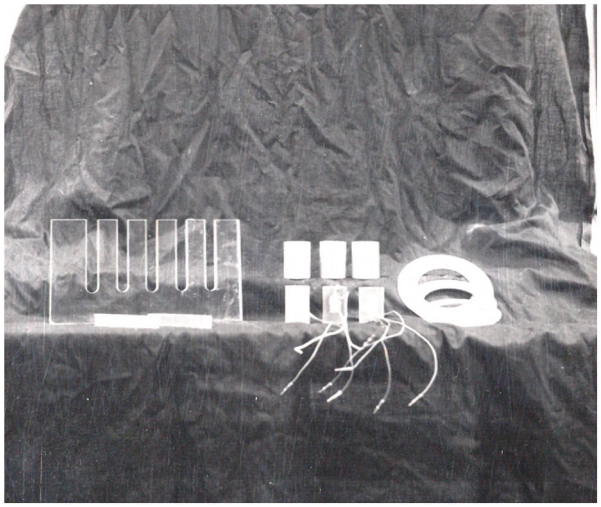

Figure 18. Plastic specimens and aluminum rings.

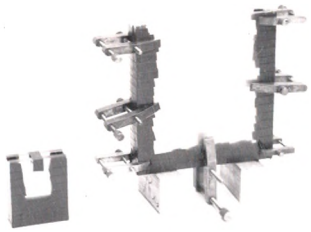

Figure 19. Molds for plastic.

based on the data presented in Figure 12, varied as curing progressed during the effective model test period, from approximately 0.29 to 0.18 and 0.32 to 0.25 for the plate and lining materials, respectively. Consequently, it was decided to investigate the maximum influence of Poisson's ratio and the possibility of ignoring its effects on the basis that the maximum differences in end results attained by the greatest expected variation of Poisson's ratio could be neglected.

Using Savin's equations for the stresses in a plate with an elastic liner subjected to uniaxial load, calculations were made for two separate assumed material conditions; one, in which Poisson's ratio was the same, 0.3 for rock and lining and, the other, in which ratios of 0.2 and 0.3, respectively, were established. The calculated differences in the resulting stresses are as follows:

Lining:

$\sigma_r$ = 8% $\sigma_\theta$ = 10% $\tau_{r\theta}$ = Negligible effect

Plate:

$\sigma_r$ = 8% $\sigma_\theta$ = 19% $\tau_{r\theta}$ = Negligible effect

These differences in stresses were assumed to be representative of the effect of variations in Poisson's ratio during the model tests performed on finite plates in a centrifuge, and serve as one limit on the possible accuracy of quantitative interpretation of the data obtained.

It was felt that an exhaustive investigation into the effects of Poisson's ratio would be highly desirable but not absolutely warranted.

## Molds

In analyzing the models photoelastically, it was necessary that their surfaces were transparent and of uniform thickness parallel to the light. To obtain models that fulfilled these requirements, lucite plates one-half inch thick and of varying height and width were used in fabricating the molds. The major advantage of lucite was that it permitted the elimination of a mold release compound and, in turn, produced better transparency of the model surfaces. Two sizes of molds were employed; a pair of lucite plates 5 by 6 inches, used to obtain a ring of epoxy resin representing the tunnel lining, and a pair of similar plates which were 10 inches square, used to cast the portion which represented the host rock (Figure 19). These plates were closed on three sides by milled lucite spacers which were one-half inch square. The vessel thus formed was then sealed with plastic tape and strengthened with C-clamps.

When a lining was used in a model, the lining preparation preceded the usual model casting by at least twelve hours, or until the curing time gave the modulus of elasticity of the lining which was desired for the specific model to be run. Once it was cast and cured, an aluminum

ring was attached to one side of the lining epoxy resin by means of double sided scotch-tape, to serve as a template in machining. Four such aluminum rings were cut from 1/16 inch sheet aluminum with varying outside diameters, from .226 inches through .904 inches, in steps of .226 inches. The inside diameter of the liner was held constant at 2.548 inches (Figure 18). The finished lining was then placed into the larger mold and positioned so that the lower outside of the lining was two inches above the mold base and midway between the edges where it was held by additional pressure applied from the outer sides of the lucite plates. An epoxy resin that was mixed to provide different final characteristics was then poured around it to represent the host rock.

## Models

When the models were prepared, air bubbles, which sometimes resulted from rapid pouring of the liquid resin, would lodge under the lining. The greater amount of these were removed by tilting the model and stirring with a long rod. Most of the remaining bubbles rose to the surface during the first hour of curing.

After curing eleven hours, the model was taken from the mold and machined to 8 7/8 inches wide by ½ inch thick

by 8 inches, or more, high, depending upon the lining thickness used. The purpose of machining the epoxy was to give an even distribution of centrifugal forces across the model, since shrinkage took place in the upper corners of the model during the first 12 hours of curing (Figure 20). After unloading, the models were kept at a constant temperature of 70 degrees for several days in order to minimize any possible creep.

## Model Holder

The model holder was designed for general use, permitting versatility as to the size, shape and loading arrangement of the model tested (Figure 21). All parts were welded to keep play and distortion at a minimum. To support the half-inch model during acceleration, the same large lucite plates, used in casting, were placed on either side of the model. Mold release material was used to lubricate the bearing surfaces on both sides and base of the model so as to eliminate any skin stresses that might develop. Aluminum plates one-half inch thick and with openings eight inches square cut in them supported the model and lucite plates. These openings made possible a clear view of any distortion taking place while loading.

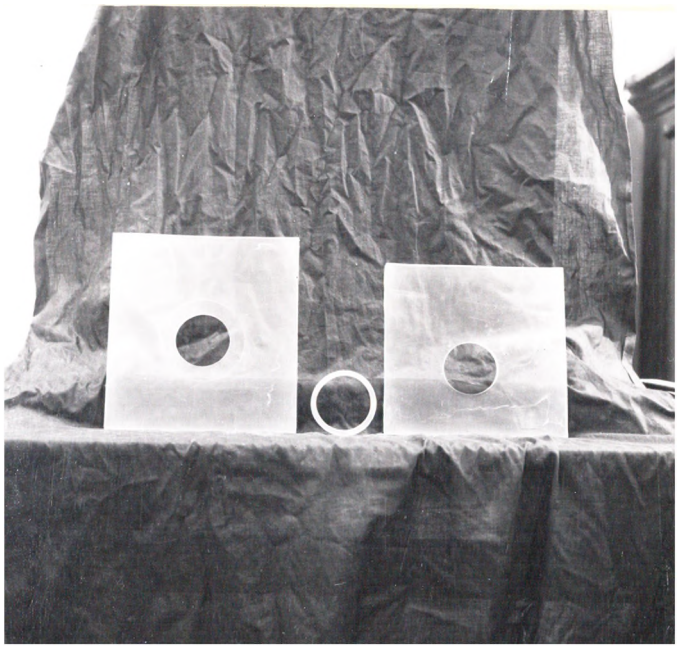

Figure 20. Models with and without lining and machined plastic lining.

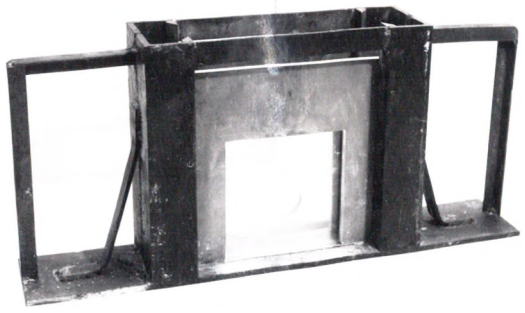

Figure 21. Model Holder with model.

All the parts were assembled in the model holder on a 1/16 inch aluminum base plate and fixed in position with spacers of fiber board and wood to make the model snug but stress-free. The assembly was then placed on a specially prepared balance and the weight of the centrifuge counter-weight adjusted until balance was achieved.

## Centrifuge

All models were loaded by means of a six foot diameter centrifuge as shown in Figure 23. A vacuum pump was used to reduce the centrifuge tank pressure by at least 20 inches of mercury before starting and then gradually reduced it another 6 inches during the first 45 minutes of operation. A stroboscopic light was located inside the tank to illuminate the model for viewing through either of two periscopes; one of which is located at the control panel and, the other, on the opposite side of the tank. A constant speed of 300 R.P.M. was reached after ten minutes of slow acceleration and held throughout the tests. The total loading time per model was held constant at four hours. The total loading time per model was held constant at four hours. At the end of each test, deceleration or the centrifuge was accomplished by a regenerative braking system using the motor and also by admitting air into the tank.

In working with models with large openings, it was found that the pressures developed by the centrifuge varied from the top to the bottom of the opening. To correct for this effect, the following formula which involves the radius distance to a particular point (Figure 22), the only varying parameter that enters the problem, was integrated between limits of a and r (i.e., the limits were obtained from the model height and the point where stress due to superincumbent material was sought):

$$W_{m_{eff.}} = \frac{4\pi^2 N^2 W_m r}{g}$$

where, $W_{m_{eff}}$ = unit weight of model under load

$r$ = radius distance to particular point

letting $C_1 = \frac{4\pi^2 W_m}{g}$ and integrating we obtain;

$$P_m = C_1 N^2 \int_a^r r\,dr = C_1 N^2 \left[\frac{r^2}{2}\right]_a^r = C_1 N^2 \left[\frac{r^2}{2} - \frac{a^2}{2}\right] = \frac{C_1 N^2}{2}\left(r^2 - a^2\right)$$

Dividing by $N^2a^2$ we have the following formula as a general case:

$$\frac{P_m}{N^2a^2} = \frac{C_1}{2}\left(\frac{r^2}{a^2} - 1\right)$$

where, $P_m$ = the uniaxial stress developed in the model. This is plotted in Figure 25 as $\frac{P_m}{N^2a^2}$ vs. $\frac{r}{a}$ from which the depth below the surface of a prototype may be determined for any given size of opening. When Figure 25 is corrected to show an approximate, constant pressure drop across the

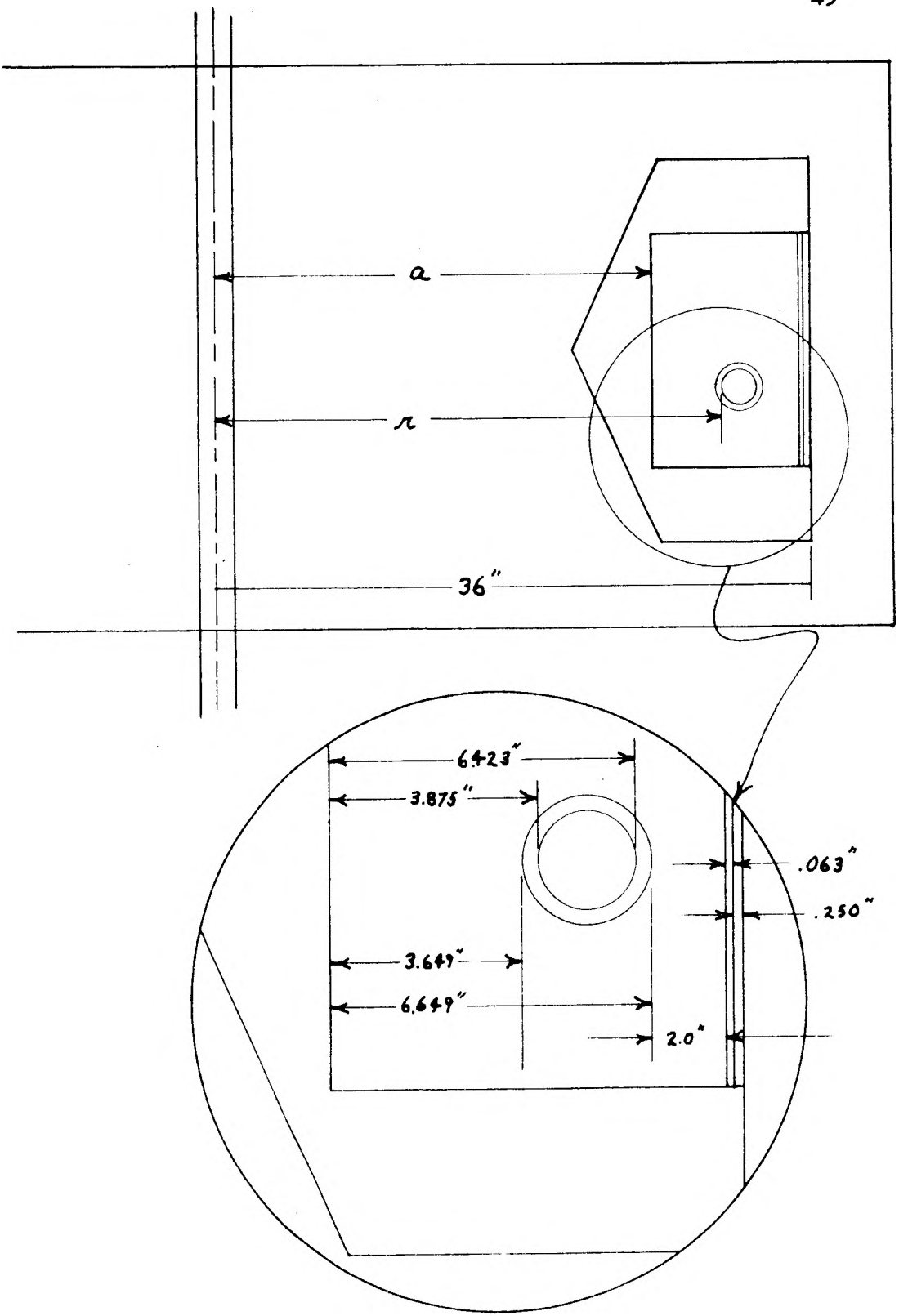


FIG. 22 Centrifuge Rotor Wing

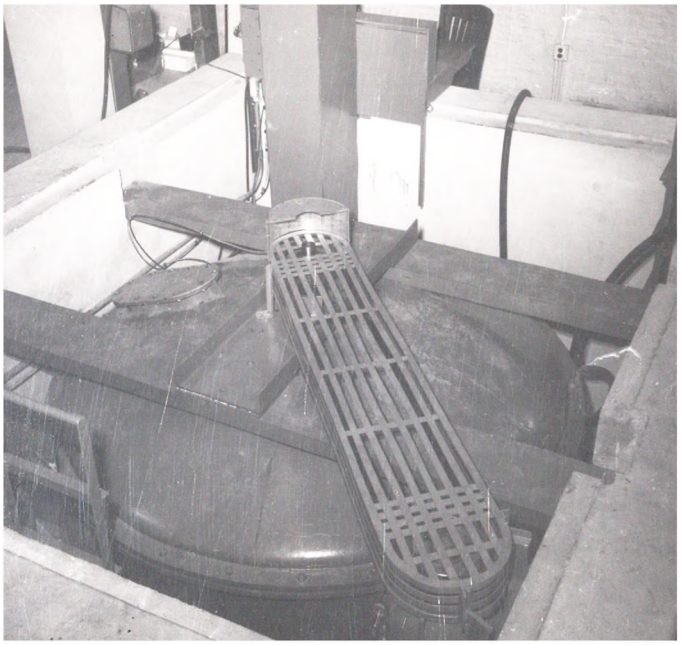

Figure 23. Centrifuge.

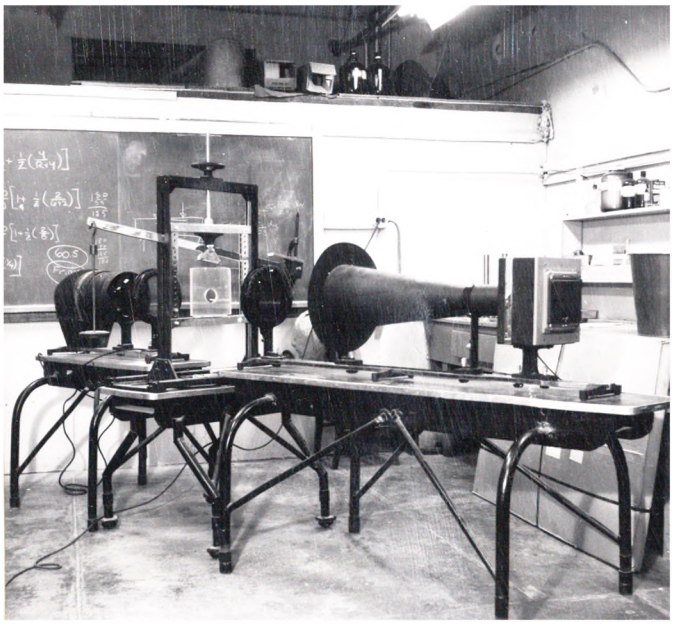

Figure 24. Polariscope.

opening, true depth of a prototype may be found by using the ratio of $\frac{h}{2r}$ (Figure 26), and by assuming a prototype radius,

where h = Depth of the opening

r = Radius of the circular opening.

In test number 7, where "a" and "r" equal 27.038 inches and 33.461 inches, respectively, for the low, inside point of the epoxy lining and "a" and "r" equal 27.038 inches and 30.913 inches, respectively, for the upper inner surface of the lining, this ratio is;

$$\frac{h}{2r} = 1.2$$

It should be noted that the effect of the radius of the centrifuge upon the pressure distribution across the opening is relatively insignificant. However, the pressure distribution obtained when models are loaded only by their own body forces is comparable only to prototype openings near the surface.

It is possible to express stresses at a point in the model in terms of stress concentration factors, based on the average stress at the mid-point of the opening. These stress concentration factors can be shown to be independent of modulus of elasticity, if the ratio between elastic moduli of composite models, and Poisson's ratios are held constant, as indicated by M. Clutterbuck[1]. That is, the relative distribution of stress throughout the model is

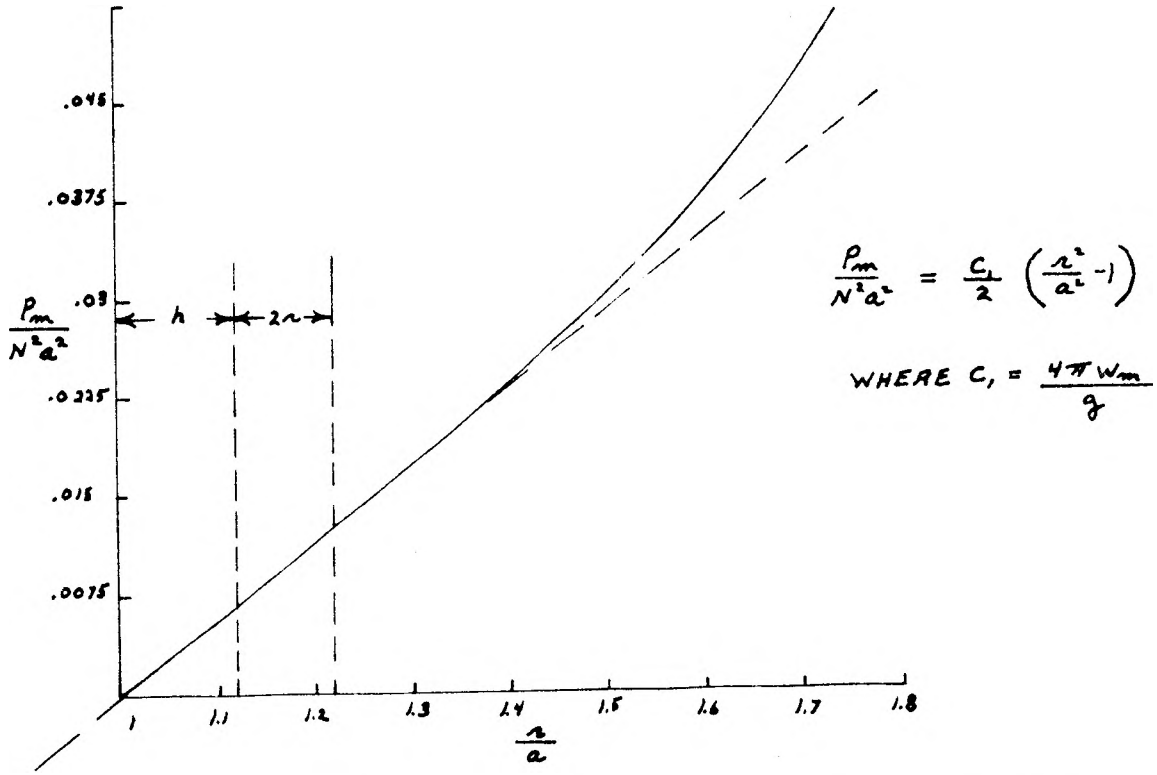


FIG. 25 Centrifuge Pressure Graph, for Epoxy Resin

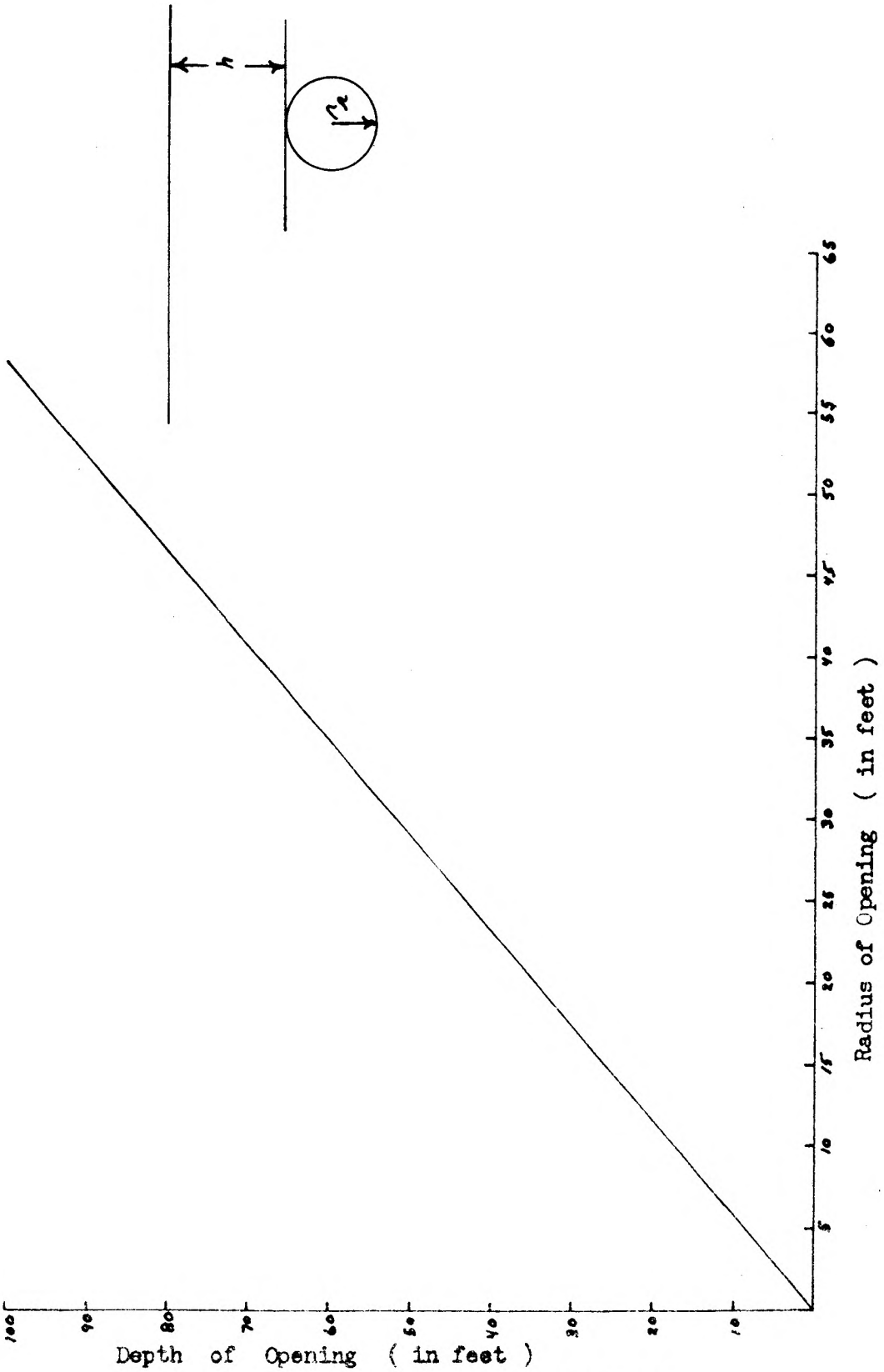


FIG. 26 Radius vs. Depth

independent of the modulus of elasticity. This behavior is illustrated by the theoretical equations developed by Savin, Figure 4, in which the ratio of stress at a point, $\sigma$, or $\rho$, to the applied uniaxial stress is shown to be independent of the rigidity and dependent on Poisson's ratio and the ratios of plate to lining rigidity for an elastic ring in a plate. It has been shown, previously in this chapter, that the effect of a change in the magnitude of Poisson's ratio of one of the components of the model has an effect which can be disregarded in approximating stress conditions around elastic liners in circular holes in plates subjected to uniaxial force. As a consequence, the expression for the stress concentration factors obtained in terms of the elastic moduli can be derived from Equation (15), giving an expression independent of model scale factor; as follows:

$$\frac{\sigma}{\sigma_o} = f_2\left[\frac{E}{E_1}, \frac{t}{R}\right]$$

## Photoelastic Procedure

The analysis of the stresses within the models were accomplished by the use of a polariscope with eight inch diameter polarizers and a monochromatic light source (Figure 24). Photographs of the isochromatic-fringe

patterns were taken with the quarter wave plates in opposition and at 45 degrees to the polarizer and analyzer so as to produce a dark field which seemed, in this case, to offer more contrast than a light field.

A relative model-fringe sensitivity of the various compositions was determined from centrally loaded, simply supported, square beams, three inches long, arranged in the manner shown in Figure 27. For each material used, the fringe order at a point directly under the load was determined as a function of time and divided into the applied load to give a relative value of fringe sensitivity, in grams per fringe. An accurate measurement of the material stress optic constant was not required since fringe values were used to compute stress concentration factors only, and all models were of the same thickness. Thus, the relative fringe sensitivity for the epoxy resin was;

$$K = \frac{P}{n'}$$

where, P = Applied load

n'= Number of fringes in calibrating beam.

Making use of the value calculated above, the relative shear stress at a point in one of the models tested in the centrifuge, was given by the expression;

$$\tau = Kn$$

where, n = Number of fringes at the point in question

K = Relative fringe sensitivity of material used

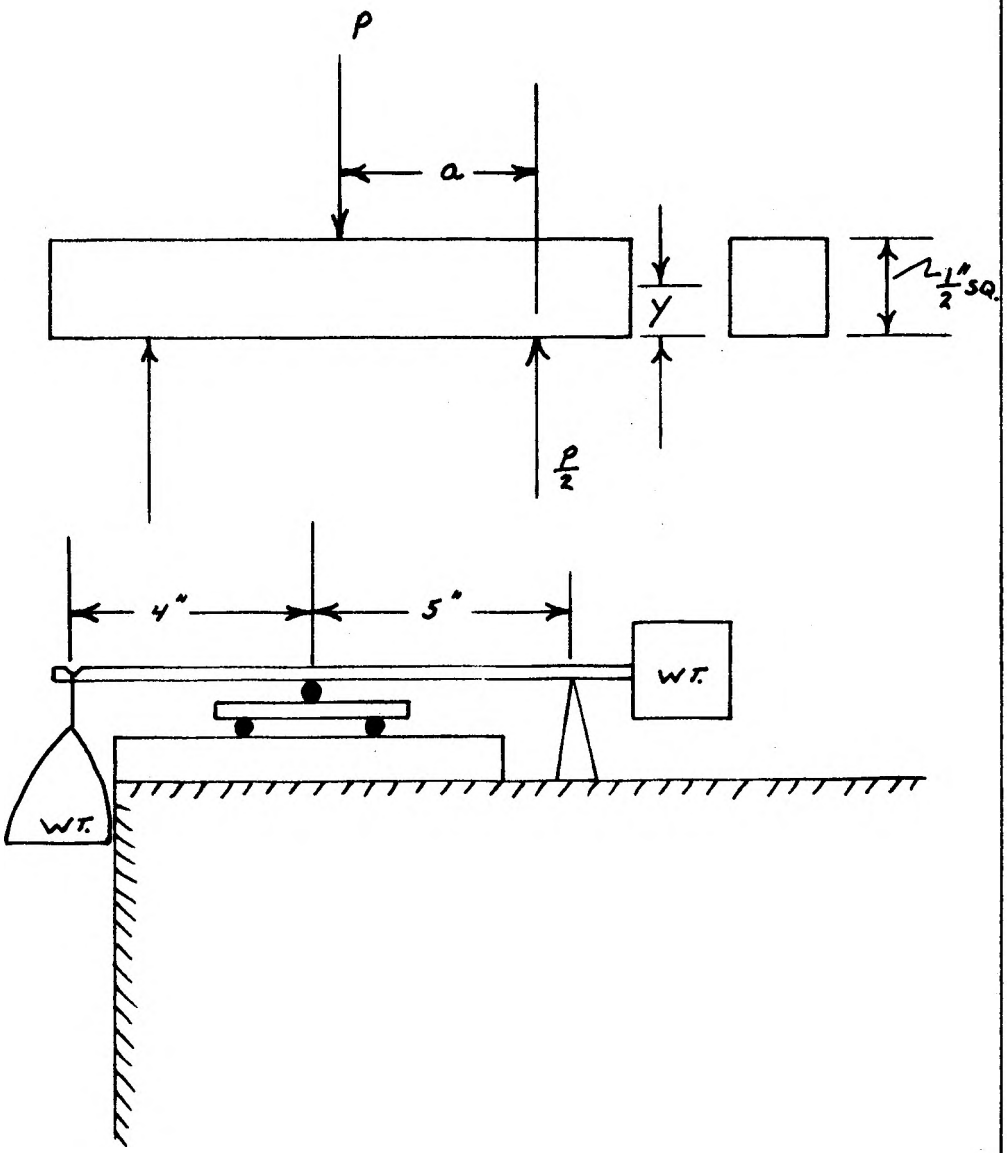


FIG. 27 Fringe Sensitivity Apparatus

Stress concentration factors at individual points around the interior of the elastic liner were computed by means of the expression;

$$S.C. = \frac{J}{J_o} = \frac{nK_1}{n_o K_p}$$

where, n = Number of fringes at point in question

$n_o$ = Number of fringes at the outer edge of the plate at the level of the hole horizontal diameter

$K_1$ = Relative fringe sensitivity of liner

$K_p$ = Relative fringe sensitivity of plate.

For example, in test 5, the shear stress concentration factor on the innermost point of the lining at the horizontal diameter was given by;

$$S.C. = \frac{14}{2} \times \frac{600}{600} = 7$$

## Test Parameters

The parameters that were varied and those held constant, are as follows:

Parameters held constant

1. Circular shaped opening
2. Induced G's on the model
3. Time under load
4. Unidirectional stress field
5. Inside diameter.

Parameters varied

1. Modulus of elasticity
2. Thickness of lining

Once these parameters were chosen, nine tests were run with one test being common to both of the two groups. This resulted in four tests with varied lining and wall rock and four tests with different lining thicknesses. Two tests were run with no lining for comparison.

# CHAPTER IV

## RESULTS AND ANALYSIS

In eight of the tests conducted, photographs were taken of the "frozen-in" stress distribution. These and their analysis are shown in Figure 28 through 35. For convenience in the analysis, these tests are grouped into three categories as follows:

1. Circular openings with no lining.
2. Circular openings with linings, but varying material characteristics.
3. Circular openings with linings of relatively the same material characteristics, but different lining thicknesses.

Each group has been analyzed for the stress intensity and the stress distribution in the plates as compared to those in the lining.

### Circular Opening with no Lining

In Figure 28B is seen the tangential stress distribution around a circular opening in a plate which has been loaded by centrifugal force. The stress trajectories in the plate around the opening are illustrated in Figure

28C. All the data were obtained from the model and Figure 28A. It should be noted that the compressive stress concentration factor at the rib of the opening was 2.8. When this is compared to the normal theoretical value of 3.0, for a circular opening in a unidirectional stress field, it indicates that the experiments were conducted with fair accuracy.

## Circular Openings with Linings, but varying Material Characteristics

Tests discussed in this sequence have been arranged in the order of increasing rigidity in the plates with respect to that of the liners. In all cases, the ratio of lining thickness to lining inner radius was held constant at $t/R = .177$.

Figure 29-A shows a rigid lining surrounded by a more flexible material. Here, the maximum stress concentration factor in the lining was 34 as compared to the free-field stress in the plate at the level of the horizontal diameter of the hole. The stress concentration factor in the plate at the end of the horizontal hole diameter was 1.0. Stress distribution in the lining is shown in Figure 29-B. As indicated, the stress concentration factors developed in the lining were the highest of

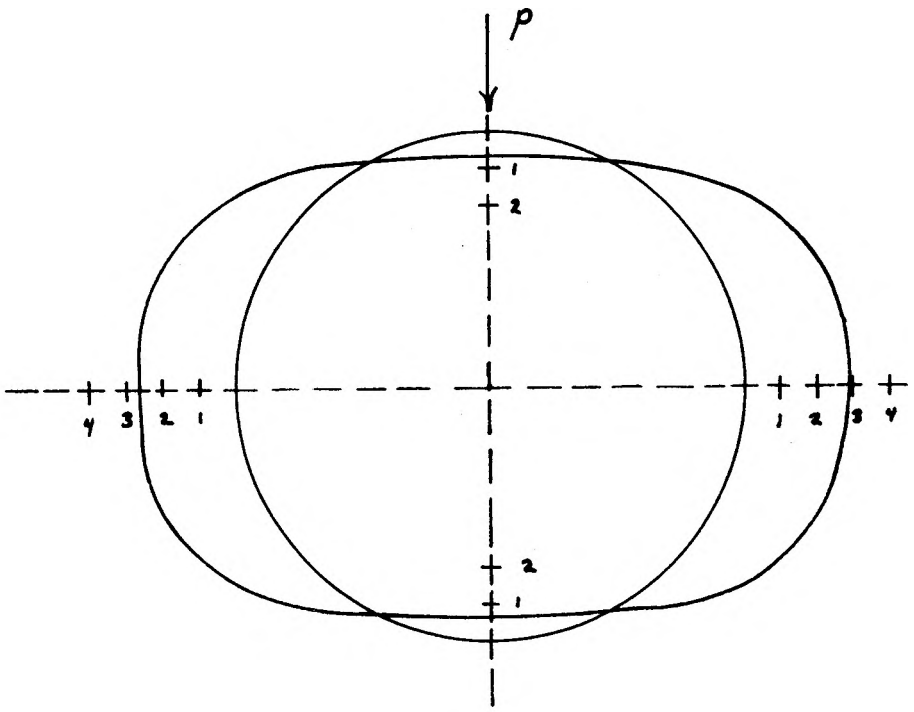


FIG. 28-B Stress Distribution Around Circular Opening

FIG. 28-A Stress Pattern of Unlined Circular Opening

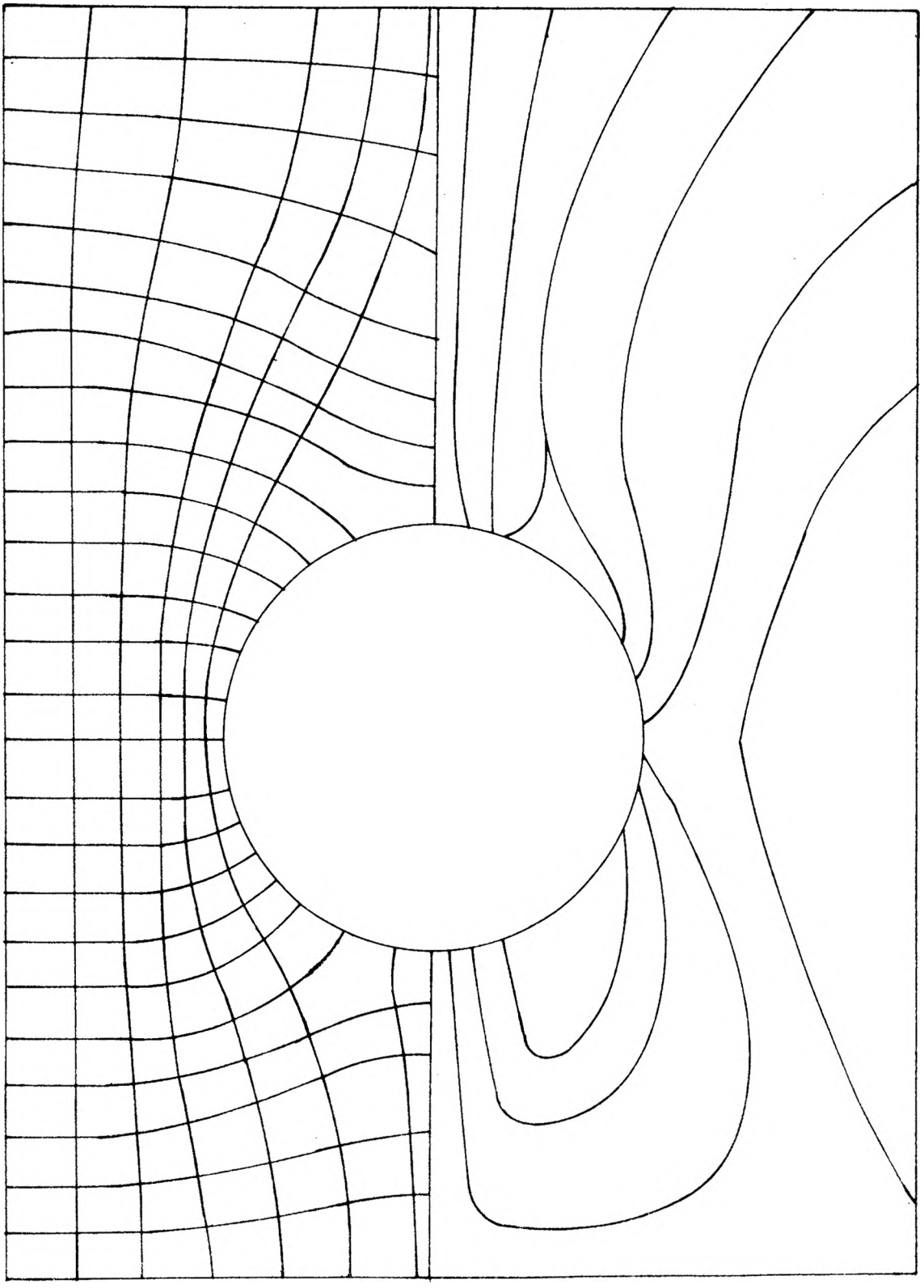

FIG. 28-C Stress trajectories and isoclinics

the entire series of tests due to the extreme flexibility of the plate.

Figure 30-A shows a model with greater relative plate rigidity than that of the previous test. In this case, the ratio of the maximum shear stress in the lining to the maximum shear stress in the plate was 7 to 1. The tangential stress distribution on the inner surface of the lining is shown in Figure 30-B. The shear stress concentration factor in the plate at the horizontal diameter was 1.3.

Figures 31-A and 32-A are photographs of fringe patterns for models with even greater relative plate rigidities. The maximum stress concentration factor obtained from Figure 31-A was 3.7. This is plotted with the stress distribution in Figure 31-B. A maximum stress concentration factor of 2.7 was obtained from Figure 32-A and it represents the model with the highest plate rigidity. The stress concentration factor in the plates at the horizontal diameter of the hole was approximately 2.0 in both cases. It should be noted that,in all cases, lining rigidity was greater than that of the plate.

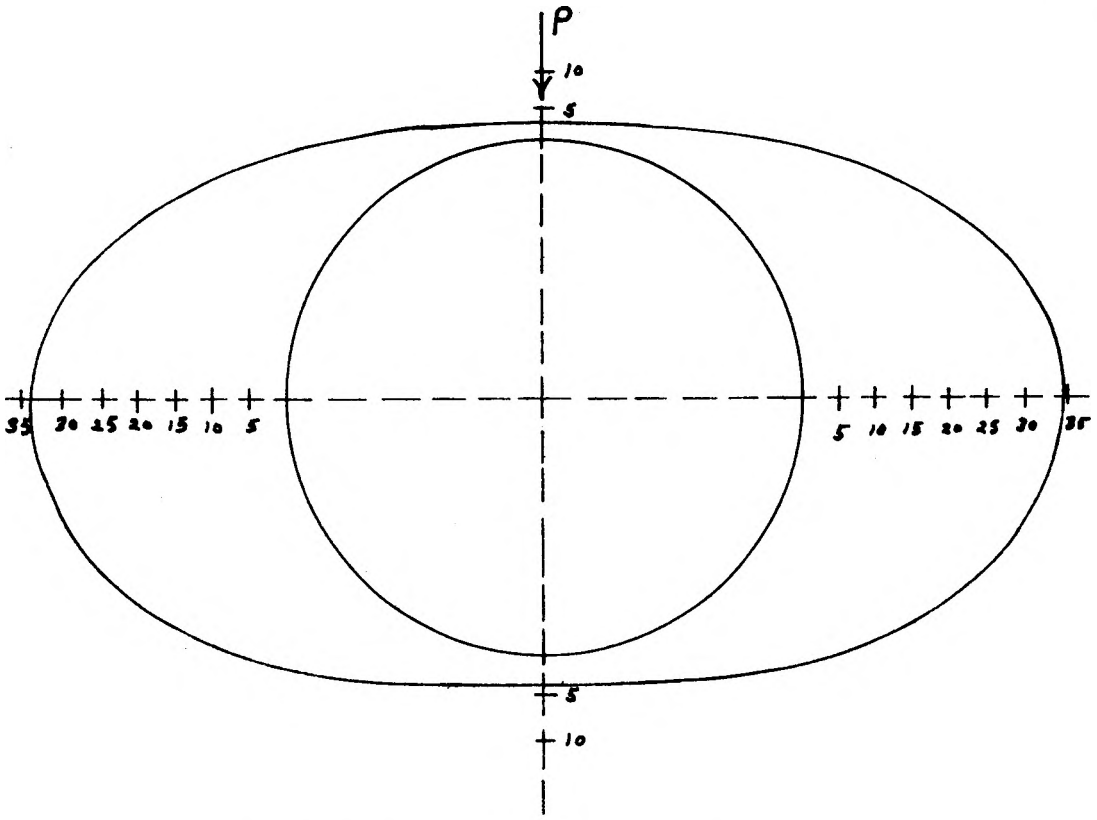


FIG. 29-B Stress Distribution in Lining

FIG. 29-A Stress Pattern of Rigid Lining and Weak Plate, t/R = .177

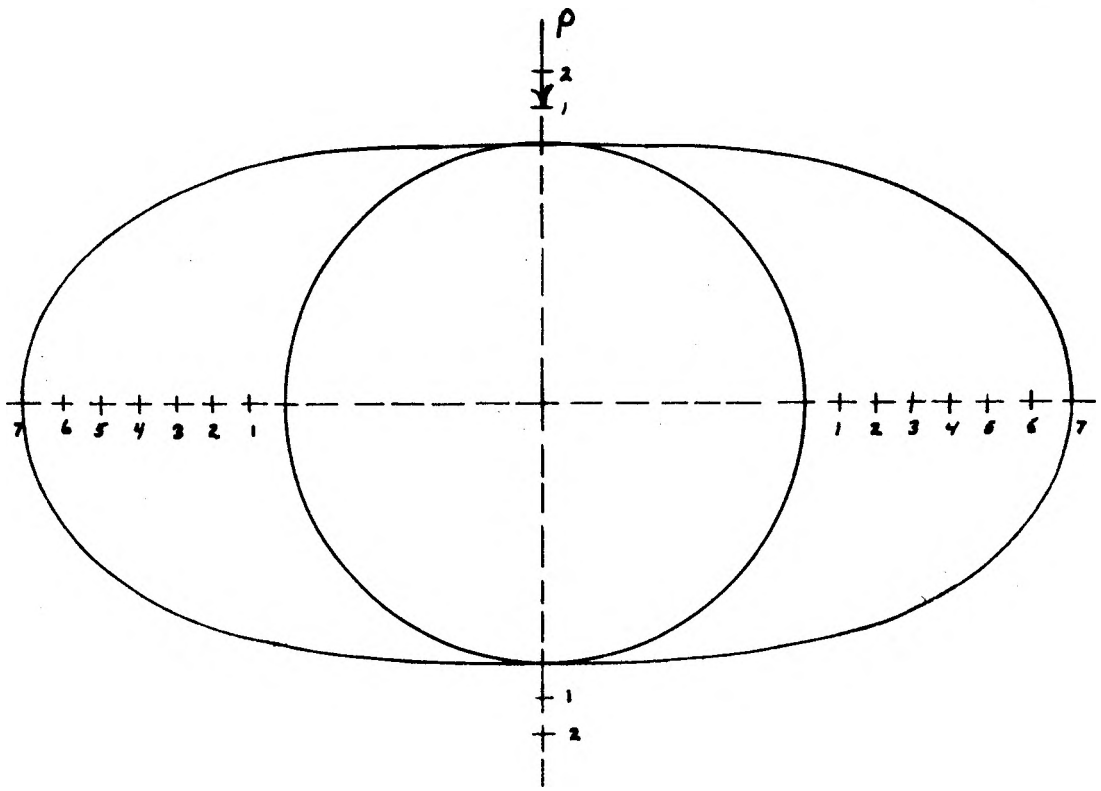


FIG. 30-B Stress Distribution in Lining

FIG. 30-A Most Rigid Lining, t/R = .177

## Circular Openings with Linings of Similar Material Characteristics, but different Lining Thicknesses

This series consisted of four tests in which the ratio of the lining thickness to lining inner radius, t/R, was varied while holding the plate and lining material properties constant.

Figure 31-A is a picture of the model with a lining thickness to radius ratio of .177, which was the lowest of the series. The stress distribution along the inner circumference of the lining is shown in Figure 31-B. In this test, the maximum stress concentration factor in the lining was 3.7. More time was taken in the test cycle of this model because it was the first to be run and, therefore, the material characteristics did vary more than those of the other three.

Figure 33-A represents a model with a lining thickness to radius ratio of .354. Here, the maximum stress concentration ratio was approximately 4.0. As can be seen, the stresses at the top and bottom of the liner were tensile instead of the compressive stresses observed in the previous model. The shear stress concentration factor of the plate adjacent to the horizontal diameter of the hole was 1.5. The lining tangential stress distribution is shown in

Figure 33-B.

Figure 34-A shows a model with a lining thickness to radius ratio of .531. The maximum stress concentration factor at the rib of the lining was 3.8, the tensil stress concentration factors at the top and bottom of the opening were almost 1.0, and the stress concentration factor at the edge of the hole in the plate was 1.2. Figure 34-B illustrates the tangential stress distribution in the lining.

Figure 35-A shows a model with a lining thickness to radius ratio of .708 and Figure 35-B outlines the stress distribution in the lining. A maximum compressive stress concentration factor of 2.5 is shown in the rib of the liner with a tensile factor of 0.3 in the bottom. The stress concentration factor in the plate at the edge of the hole was 1.1.

The results of these last four tests are presented graphically in Figure 36 which shows the stress plotted against the ratio of the thickness of the liner over the lining inner radius.

A condition of uni-axial compression applied to a plate containing a circular hole and into which an elastic ring is inserted was mathematically analyzed by Savin. Two of his five conclusions were substantiated photoelastically in this study. From the data summarized in Figure 36, and the discussion above it has been shown that:

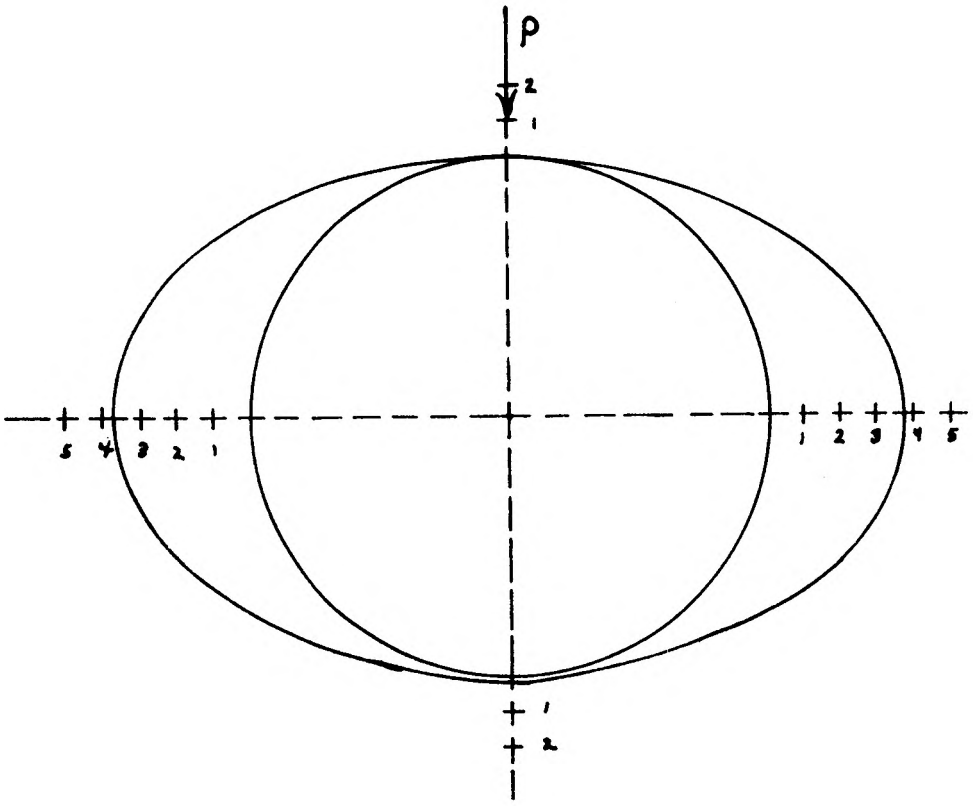


FIG. 31-B Stress Distribution in Lining

FIG. 31-A Thinnest Lining in Series of Lining Thicknesses, t/R = .177

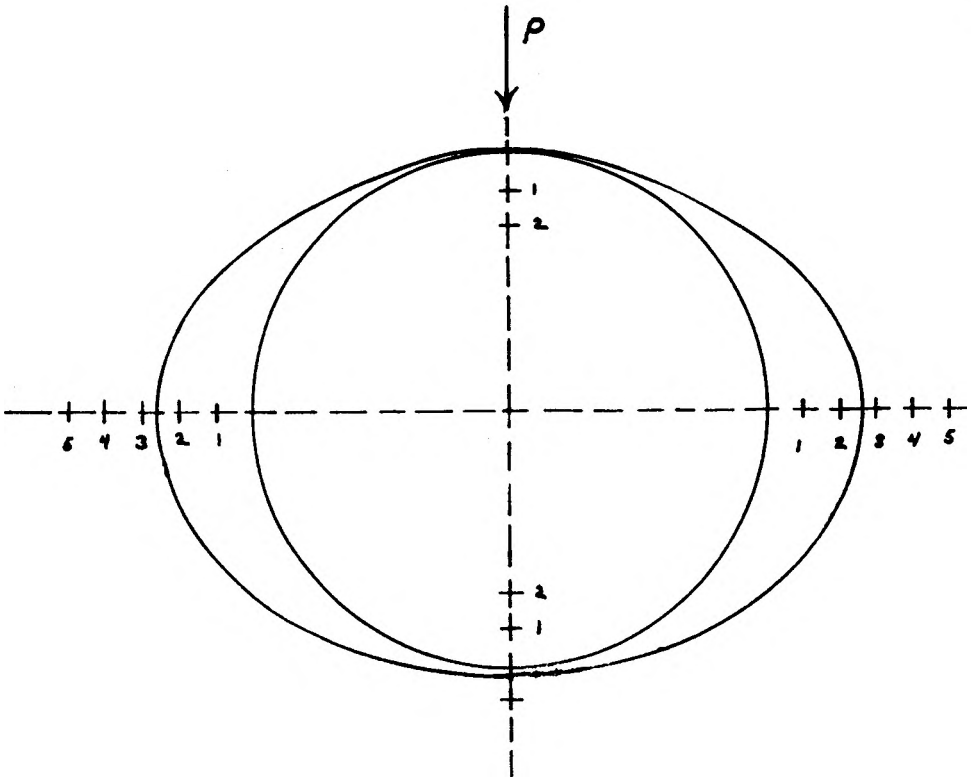


FIG. 32-B Stress Distribution in Lining

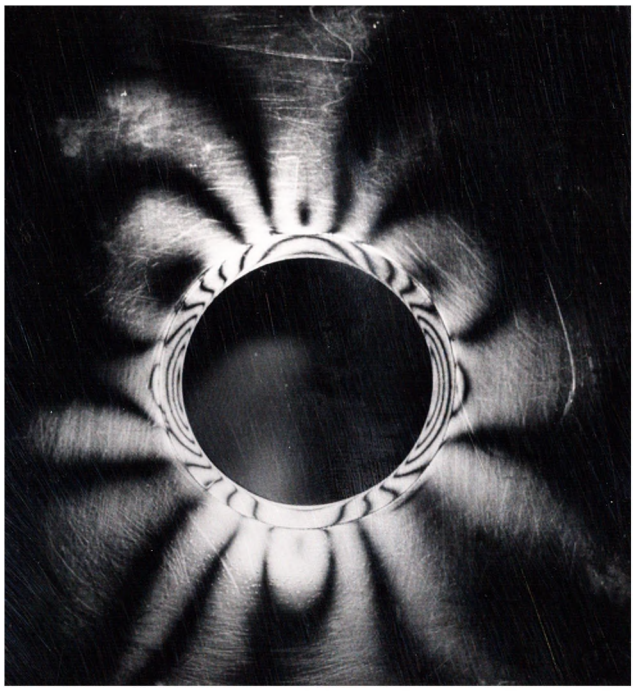

FIG. 32-A Least Rigid Lining, t/R = .177

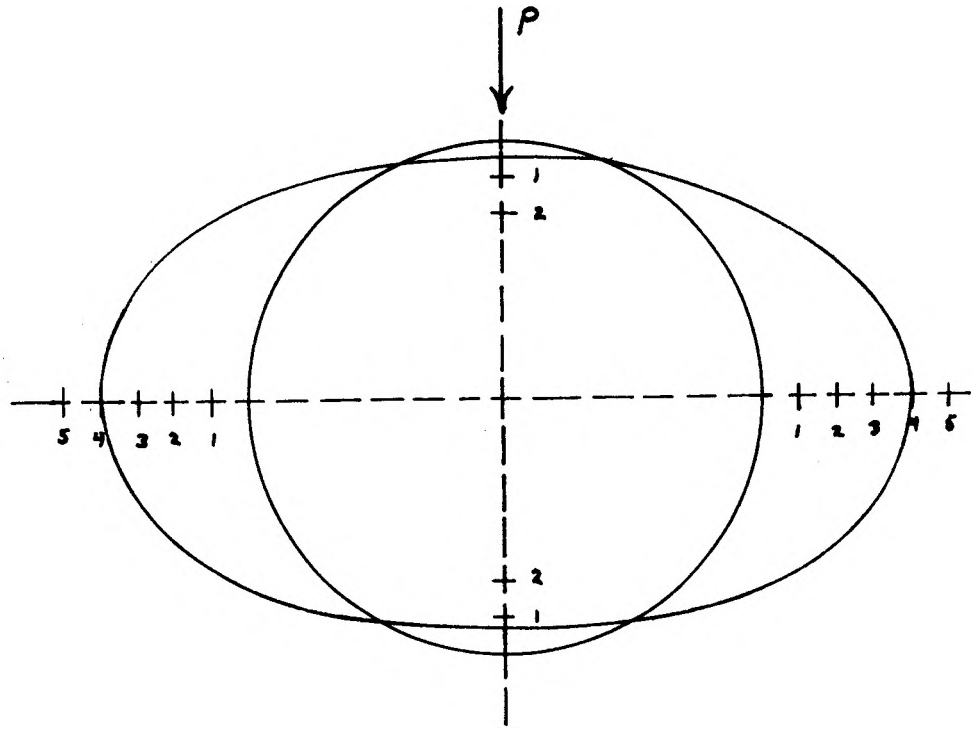


FIG. 33-B Stress Distribution in Lining

FIG. 33-A Lining Thickness of .452 inches,
t/R = .354

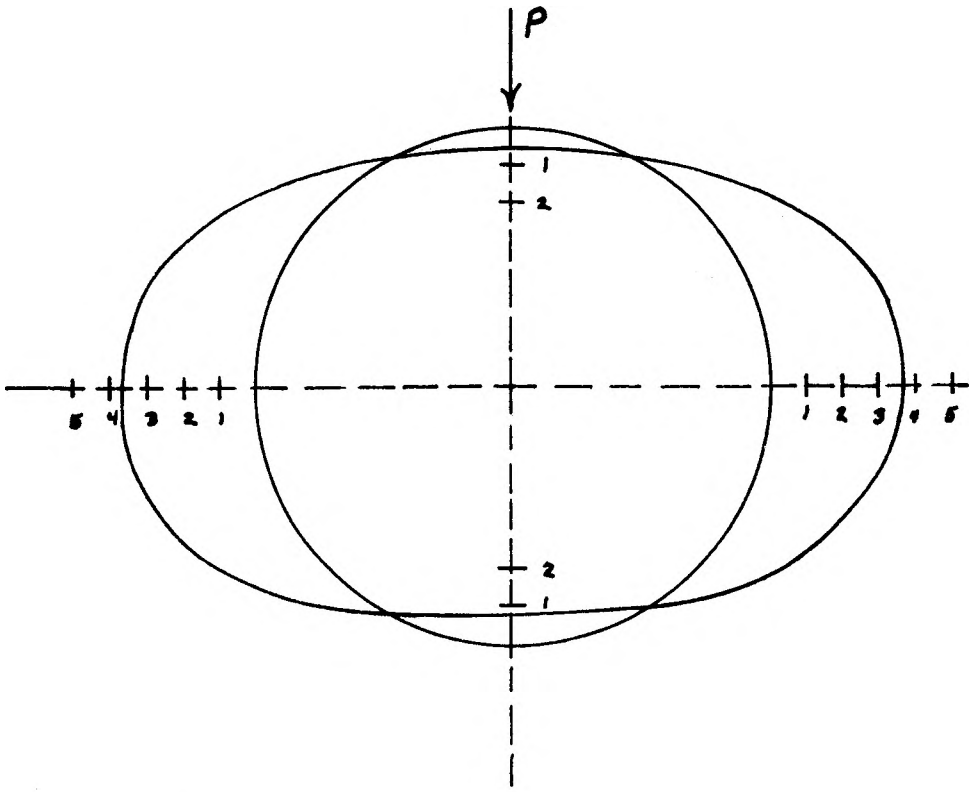


FIG. 34-B Stress Distribution in the Lining

FIG. 34-A Lining Thickness of .678 inches, t/R = .531

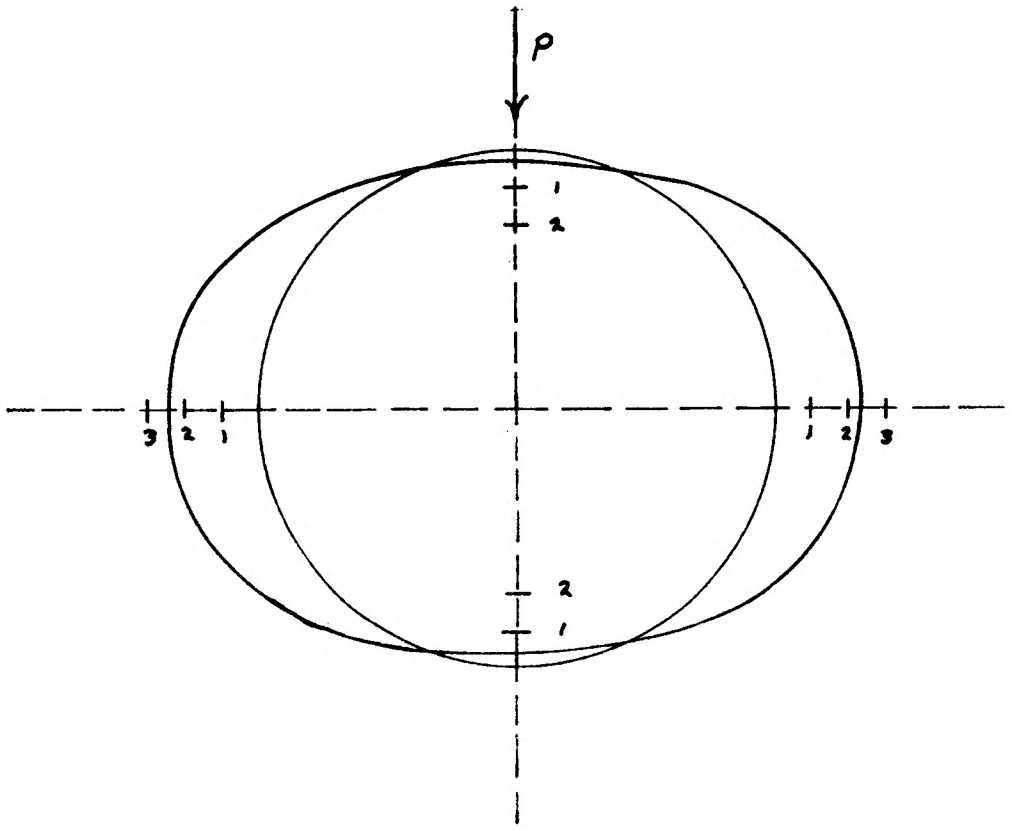


FIG. 35-B Stress Distribution in Lining

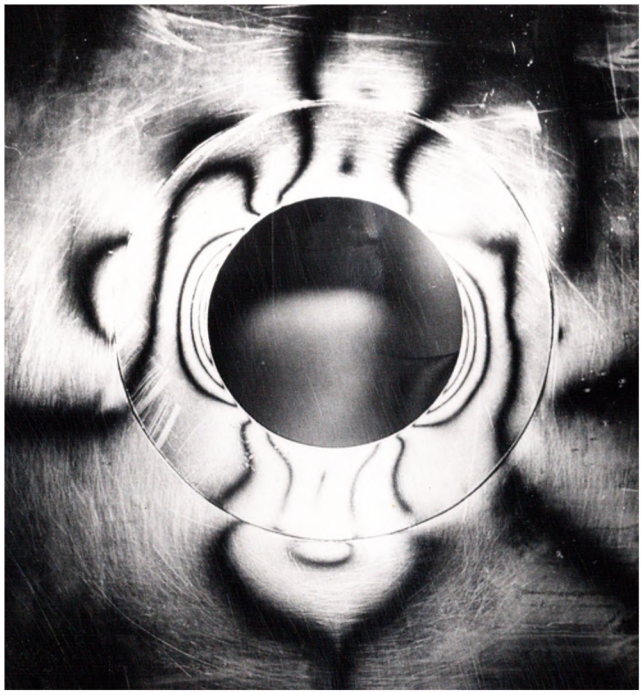

FIG. 35-A Lining Thickness of .904 inches,
t/R = .708

1. With decreasing ratio of rigidity of plate to the rigidity of the ring, the stress concentration in the plate decreases while the tangential stress in the ring increases.
2. With increasing thickness to radius ratio of a relatively rigid ring, the stress diminishes both in the ring and in the plate.

The models shown in Figures 29-A, 30-A, 31-A and 32-A (varying ratios of elastic moduli) show a very definite influence of the rigidity of the lining used. The plate material represented in Figure 29-A had a prolonged curing cycle which permitted the stress to creep out to a much greater extent than had been experienced in any of the other tests. These tests offer verification of Savin's first point.

In the models shown in Figures 31-A, 33-A, 34-A, and 35-A (varying liner thicknesses to radius ratios) the stress concentration shows a decrease in the lining as well as in the wall rock with an increase in the ratio. Figures 31-A (ratio of 0.177) and Figure 35-A (ratio of 0.708) illustrate this clearly, as they are extreme examples.

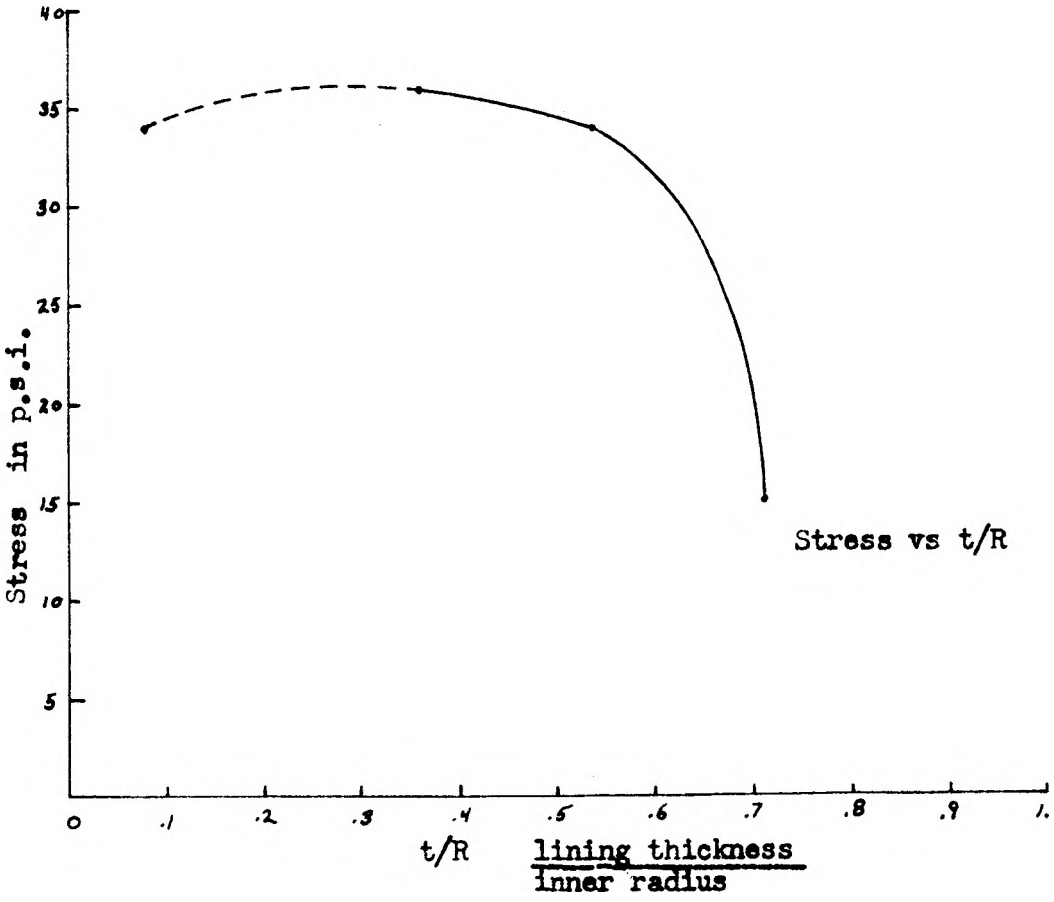


FIG. 36 Stress vs. Lining Thickness to Inner Radius Ratio

# CHAPTER V

## SUMMARY AND CONCLUSIONS

Methods and techniques have been developed for preparing, loading and analyzing, suitable photoelastic models of tunnel linings, surrounded by materials of different physical properties to represent host rocks. The models were stressed in a centrifuge to simulate a condition that would exist in shallow underground tunnels, in order to study the influence of various lining conditions upon the stress distribution.

The following new techniques were established in order to expedite this study:

1. Different material characteristic curves for three compositions of epoxy resin were developed. These curves showed the instantaneous values of the varying elastic properties of the resins at any time during the curing period.

2. Calculation of the data for a graph which was used for computing the pressure drop across large openings while being loaded in the centrifuge. This lead to a more rapid calculation and it simplified the analysis.

3. The development of a method to load large plates of epoxy resin in the centrifuge with negligible skin

stresses. In this way, a photoelastic analysis of the "frozen-in" stress was achieved.

From the photoelastic analyses conducted and in agreement with the results obtained from a mathematical solution presented by Savin, it is seen that the stress decreases in the host rock as well as in the lining when the lining thickness to radius ratio becomes greater. When the lining becomes more rigid than the surrounding rock, there is a higher concentration of stress in the lining. From this analysis, it would seem that a lining that is thick and less rigid would be stressed the least. To summarize:

1. With increasing rigidity of the ring, the stress concentration in the plate decreases although the tangential stress in the ring increases.

2. With increasing width of a relatively rigid ring, the stress diminishes both in the ring and in the plate.

The centrifuge is an excellent means of loading epoxy resin models when applying the "stress freezing" method for stress distribution studies. The technique can be facilitated even further through the use of graphs and calculations such as those employed in this study.

# RECOMMENDATIONS FOR FURTHER STUDY

There are several aspects of tunnel linings yet to be investigated. Some further work that might be done is listed below:

1. The analysis of different shaped openings containing linings.

2. The analysis of a combination of two or more linings, cast in one model opening but with differing material characteristics.

3. Varying thicknesses at different points in the lining.

4. The effects upon stress distribution when the conditions at the interface of the lining and rock are changed.

5. Photoelastic study of wall rock destressing techniques, using a lining to evaluate the decrease in stress.

6. A study of the effect of Poisson's ratio on the stress distribution in a plate of two different epoxy resins during the curing time.

7. A study to determine more exacting values for the modulus of elasticity of epoxy resins, while curing under load.

All of the above studies are certain to contribute toward improving the design of underground mine openings

and, it appears, that all of them may be conducted by utilizing the techniques outlined herein.

# BIBLIOGRAPHY


1. Clutterbuck, M., 1958, "The Dependence of Stress Distribution on Elastic Constants" British Journal of Applied Physics, Vol. 9, P.P. 323-329.

2. Dally, J. W., Durelli, A. J. and Riley, W. F., March 15, 1957, "A New Method to 'lock-in' Elastic Effects for Experimental Stress Analysis", Journal of Applied Mechanics, Paper No. 57, A-71.

3. Galanka, J., 1959, "Problems of Shaft Sinking in Poland", Symposium on Shaft Sinking and Tunnelling, The Institution of Mining Eng.

4. Gibson, W. L., April 1956, "Some Experiences in Investigating Stresses and Forces in Massive Structures", Canadian Mining and Met. Bulletin, P.P. 241-253.

5. Haber, D., 1962, "A Study of the Stress Distribution Around Circular Openings using Multilayered Photoelastic Material", M.S. Thesis Mining Dept. M.S.M.

6. Hetenyi, M., March 1954, Handbook of Experimental Stress Analysis, Published by John Wiley & Sons, Inc., Second Printing.

7. Hiramatsu, Y., Oka, Y., Ogino, S., Memoirs, January 1961, "Investigations on the Stress in Circular Shaft Linings", Fac. Eng., Kyoto Univ. Vol. XXIII/I.

8. Hogg, A. D., May 1959, "Some Engineering Studies of Rock Movement in the Niagara Area", Engineering Geology Case Histories No. 3, Symposium on Rock Mechanics.

9. Isaacson, E. De St. Q., 1958, "Rock Pressure in Mines", Mining Publications, Ltd. Salisbury House, London, E.C.2.

10. Moody, W. T., May 1959, "Importance of Geological Information as a Factor in Tunnel-Lining Design", Engineering Geology Case Histories No. 3, Symposium on Rock Mechanics.

11. Moye, D. G., May 1959, "Rock Mechanics in the Investigation and Construction of T.1 Underground Power Station, Snowy Mountains, Australia", Engineering Geology Case Histories No. 3, Symposium on Rock Mechanics.

12. Obert, L., Duvall, W. I., Merrill, R. H., 1960, "Design of Underground Openings in Competent Rock" Bureau of Mines Bulletin 587.

13. Panek, L. A., 1951, "Centrifugal Testing Apparatus for Mine-Structure Stress Analysis", Bureau of Mines R.I. 4883.

14. Roux, J. A., Denkhaus, H. G., Leeman, E. R., 1956, "The Stresses in, and the Condition of the Ground Around, Mining Excavations", Trans. of the Canadian Inst. of Min. & Met. and of the Min. Soc. of Nova Scotia Vol. LIX.

15. Savin, G. N., 1961, "Stress Concentration Around Holes", Pergamon Press, P.P. 234-242.

16. Shepherd, R., Wilson, A. H., 1959-60, "The Measurement of Strain in Concrete Shaft and Roadway Linings", I.M.E. Trans. P.P. 561-77.

17. Shimada, H., 1961, "Influence of Breadth in Bars with Reinforced Circular Holes Under Tension", Experimental Mechanics" P.P. 33-39.

18. Spalding, J., 1949, "Ground Control-Theory and Practice", Inst. of Min. and Met. Bulletin No. 507, P.P. 1-35.

19. Tomkins, G., 1956-57, "Some Features of Shaft Sinking and Inset Work at Cynheidre", I.M.E. Trans. P.P. 672-709.

20. Walker, S., 1920, "Modulus of Elasticity of Concrete", Structural Materials Research Lab., Lewis Inst., Chicago, Bulletin 5 P.P. 1-78.

21. Wood, A. F., 1956-57, "Placing of Mass Concrete Shaft Lining in Frozen Ground", I.M.E. Trans. P.P. 714-27.

# VITA

Martin Samuel Oudenhoven was born June 30, 1927, at Waukesha, Wisconsin. His elementary education was received in a country school in Waukesha County and he was graduated from the Waukesha High School in 1945. After returning to the United States at the end of military service in Europe, he married Madeleine Soddu.

In September 1947, he enrolled at Wisconsin Institute of Technology at Plattville, Wisconsin, and received a diploma for the three-year course in mining engineering, after which time he transfered to the Missouri School of Mines and Metallurgy to receive his B.S. degree in Mining Engineering in the spring of 1951.

Two years were spent on a training program for Kennecotte Copper Corp., at Bingham Canyon, Utah. He later went to South America to work for Cerro De Pasco Corp. in their mine at Casapalca and, later, Cerro De Pasco, Peru.

In September 1961, he enrolled at the Missouri School of Mines and Metallurgy to do graduate work toward the degree of M.S. in Mining Engineering.


MISSOURI SCHOOL OF MINES & M T
LIBRARY
105465
JAN 22 1963
ROLLA,